TAMPEREEN TEKNILLINEN YLIOPISTO
TAMPERE UNIVERSITY OF TECHNOLOGY

ELISA KOPONEN

PROPERTIES AND BEHAVIOUR OF SWITCHABLE ADHESIVE

Master of Science Thesis

Examiner: Prof. Jurkka Kuusipalo
The examiner and topic of the thesis were approved by the Council of the Faculty of Engineering Sciences on 4th March 2015

ABSTRACT

ELISA KOPONEN: Properties and Behaviour of Switchable Adhesive
Tampere University of Technology
Master of Science Thesis, 67 pages
June 2015
Master's Degree Programme in Material Science
Major: Technical Polymer Materials
Examiner: Professor Jurkka Kuusipalo

Keywords: switchable adhesive, flexible display, PEN substrate

The flexible displays technologies have experienced an increased interest in recent years. The producing of OLED technology on the flexible substrate has however been a problem due to the precision required during the assembly of multiple layers that make up an OLED structure. One solution is to use the same manufacturing technique as for glass substrate, utilising switchable adhesive between the flexible substrate and glass, which in this case work as a carrier. After the electronics have been manufactured, the flexible substrate is peeled away and the adhesive remains bonded to the glass after high temperature heating. The purpose of this thesis is to study and characterise the properties and the behaviour of the adhesive that switches off and on when heat is applied.

The properties of the switchable adhesive change when it is cured at different temperatures. To study the changes, the adhesive coated on PEN film was laminated on to microscope glass slide to and then tested after curing the laminates in an oven or on a hotplate at different temperatures and curing times. The surface properties of the adhesive such as the surface energy and Fourier transform infrared absorption were measured for the adhesive remaining on the glass slide and also the adhesive on PEN film prior to lamination. The peel strength between PEN film and adhesive was studied with 90° peel test. The thermal properties of adhesive were evaluated with DSC and TMA techniques.

The adhesive was seen to switch from PEN film to glass slide after it was cured at 80 °C and peeled. The surface energy of the adhesive was studied before and after the switch and it was found that the surface energy changes from 50 dynes/cm, which is close to surface energy of PEN film, to 70 dynes/cm, which is close to surface energy of glass, after the curing temperature increased to 80 °C. This change could not be seen with the FTIR, but it showed another change after curing the laminate for 2 minutes at 160 °C. From the peel tests the second change was seen to start already at 140 °C and it was seen that this change occurs faster with higher curing temperatures. This indicated that a clear reaction is occurring in the adhesive when heated. The change at higher temperatures was also detected with DSC, which showed an irreversible reaction after the sample was first heated to 120 °C. The change at higher temperatures was most likely due with the crosslinking and degradation. The degradation was also seen as a bubbling in the laminate when the curing temperature increased to 180 °C. To characterise the reaction further, the reaction kinetics was calculated based on FTIR analysis.

TIIVISTELMÄ

ELISA KOPONEN: Vaihtuvan adhesiivin ominaisuudet ja käyttäytyminen
Tampereen teknillinen yliopisto
Diplomityö, 67 sivua
Kesäkuu 2015
Materiaalitekniikan diplomi-insinöörin tutkinto-ohjelma
Pääaine: Tekniset polymeerimateriaalit
Tarkastaja: professori Jurkka Kuusipalo

Avainsanat: vaihtuva adhesiivi, taipuvat näytöt, PEN substraatti

Joustavat OLED näytöt ovat kasvattaneet kiinnostusta viime vuosina. OLED teknologian valmistaminen joustavalle substraatille on kuitenkin osoittautunut haasteelliseksi, johtuen monikerroksisen OLED rakenteen vaatimasta tarkasta asennuksesta. Yksi vaihtoehto on käyttää samaa valmistusmenetelmää kuin lasinäytöissä, kiinnittämällä joustava substraatti lasiin vaihtuvan adhesiivin avulla. Tällöin lasi toimii vain alustana valmistusprosessin ajan. Kun elektroniikka on asennettu, joustava näyttö voidaan repäistä pois lasialustasta. Lämpökäsittelyn takia vaihtuva adhesiivi on tarttunut lasialustaan, joten se ei jätä jälkiä lopulliseen tuotteeseen. Tämän työn tarkoituksena on tutkia ja karakterisoida lämmöstä vaihtuvan adhesiivin ominaisuuksia ja käytöstä.

Vaihtuvan adhesiivin ominaisuudet muuttuvat, kun sitä on käsitelty eri lämpötiloissa. Jotta ominaisuuksien muutosta voitiin tutkia, adhesiivi pinnoitettiin PEN filmille ja laminoitiin mikroskoopin aluslasille. Valmiit laminaatit lämpökäsiteltiin joko uunissa tai lämpölevyllä eri lämpötiloissa ja käsittelyajoissa riippuen testausmenetelmästä. Adhesiivin pintaominaisuudet, kuten pintaenergia ja Fourier muunnos infrapuna absorptio, mitattiin lasiin siirtyneestä adhesiivista ja myös PEN filmille pinnoitetusta adhesiivista ennen laminointia. PEN kalvon ja adhesiivin välinen repäisylujuus mitattiin 90 asteen kulman repäisykokeella. Lisäksi adhesiivin termisiä ominaisuuksia arvioitiin DSC ja TMA tekniikoilla.

Adhesiivin huomattiin kiinnittyvän repäisyvaiheessa PEN filmiltä lasiin, kun laminaattia oli lämpökäsitelty yli 80 °C:ssa. Adhesiivin pintaenergia mitattiin ennen ja jälkeen adhesiivin vaihtumisen. Adhesiivin pintaenergia oli 50 dynes/cm, kun adhesiivi oli käsitelty alle 80 °C:ssa. Pintaenergian huomattiin kasvavan 70 dyneen/cm, kun käsittelylämpötila kasvoi yli 80 °C:een. FTIR mittaukset osoittivat toisen muutoksen tapahtuvan, kun laminaatti oli käsitelty yli 160 °C:ssa. Laminaatissa huomattiin myös kuplimista, kun käsittelylämpötila nousi 180 °C:een. Kuplimisen todettiin johtuvan todennäköisesti hiilidioksidin höyrystymisestä. Repäisykokeet osoittivat myös adhesiivin muuttumisen korkeammissa lämpötiloissa ja muuttumisen huomattiin olevan reaktio, joka tapahtuu sitä nopeammin, mitä korkeampi käsittelylämpötila on. Sama reaktio havaittiin myös DSC mittauksissa, jotka osoittivat irreversiibelin reaktion 120 °C:een jälkeen. Korkeammissa lämpötiloissa tapahtuvan muutoksen todettiin olevan ristisilloittumisen ja hajoamisen seurausta. Tämän reaktion kinetiikka laskettiin FTIR mittausten avulla.

PREFACE

This Master of Science Thesis was completed for DuPont Teijin Films Ltd, at Wilton headquarters, United Kingdom. Some of the research was carried out at Intertek MSG Ltd. The project was funded by DTF, but also the International Office of Tampere University of Technology sponsored this thesis. I want to express my appreciation for their financial support.

In particular I wish to express my deepest gratitude to my industrial supervisor Dr. Duncan MacKerron for his advice, professional guidance and encouragement throughout the duration of the project. I also thank Prof. Jurkka Kuusipalo from Tampere University of Technology for examining this thesis and recommending me for this position at DTF. My thanks also belong to Intertek MSG Ltd. in the Wilton Centre who performed some of the research.

In Wilton, United Kingdom, on 18 May 2015

Elisa Koponen

CONTENTS

LIST OF SYMBOLS AND ABBREVIATIONS

ATR	attenuated total reflectance
CO_2	carbon dioxide
CTE	coefficient of thermal expansion
DSC	differential scanning calorimetry
FTIR	Fourier transform infrared
IR	infrared
LED	light emitting diode
MD	machine direction
OLED	organic light emitting diode
PEN	poly(ethylene naphthalate)
PET	poly(ethylene terephthalate)
PSA	pressure-sensitive adhesive
St Resid	standardized residual
T_g	glass transition temperature
T_m	melting temperature
TD	transverse direction
TFT	thin film transistor
TMA	thermomechanical analysis

A	frequency factor
[A]	concentration of component A
$[A_0]$	concentration of A after time 0
Abs	absorbance
c	concentration
c_p	specific heat capacity (at constant pressure)
ΔP	difference in thermal power
ΔT	change in temperature
ε	Beer-Lambert absorption coefficient
E_a	activation energy
γ	surface tension (w.r.t. liquid), surface free energy (w.r.t. solid)
H	enthalpy
k	rate constant of the reaction
λ	wavelength
l	thickness of material
m	mass of the sample
n	wavenumber
N_A	Avogadro constant
π_S	spreading pressure of the adsorbing vapour
Q	heat flux
R	universal gas constant
r_A	the rate of reaction
θ	contact angle on a solid surface
v	heating rate
W_{AB}	work of adhesion
y	reference variable

Superscript

^{d}	dispersion component
^{p}	polar component

Subscript

$_{S}$	solid phase
$_{L}$	liquid phase
$_{V}$	vapour phase
$_{a}$	phase a
$_{b}$	phase b

1. INTRODUCTION

Flexible organic light emitting diode (OLED) displays are a rapidly developing technology with a potential to completely revolutionise the display markets. Poly(ethylene naphthalate) (PEN) film is used as a flexible substrate in flexible OLED displays and lighting applications due to its excellent mechanical and thermal properties as well as its high transmittance which are vital requirements for any substrate in these types of products. However, the fabrication of the OLEDs on the PEN film is a challenge and that is why glass carrier is used to obtain proper planarity and dimensional stability during manufacturing. The switchable adhesive is needed to attach the PEN film to glass carrier while the fabrication of electronics takes place. During the manufacturing heat is applied and the adhesive switches on the glass carrier and the final product can be peeled away from the glass support with the adhesive remaining on the glass. The purpose of this thesis is to study and characterise the properties and the behaviour of one switchable adhesive that is proprietary product, as switchable adhesive's performance was not understood before this study.

One of the aims was to study the surface properties of the adhesive in order to understand why adhesive switches after heating and what could be causing the transition. The studied adhesive was initially coated on PEN film and this was then laminated onto a glass microscopy slide. The surface properties were studied by calculating the surface energy of the adhesive from contact angle measurements and by using Fourier transform infrared measurements. The adhesion with PEN film after laminating and curing was studied by measuring the peel strength with 90° peel test. To understand more about the adhesive behaviour after it is cured in different temperatures the thermal analysis was undertaken. The differential scanning calorimetry and thermomechanical analysis was used for these measurements. In addition, to find at which curing temperatures and times the adhesive can be processed, the reaction kinetics were calculated.

In this thesis Chapter 2 introduces the properties, manufacturing and applications of PEN film as the adhesive studied in this work is coated on PEN film. Chapter 2 provides information about the theory of adhesives generally and with main focus on pressure-sensitive adhesives and switchable adhesives. The applications where the studied adhesive is used include flexible electronics, flexible OLED displays and flexible lighting. These are also outlined in Chapter 2, together with the specific requirements of the adhesive. Chapter 3 goes through the materials used in the study and the theory of experimental devices. Also the chapter offers information about sample preparation for each experiment. In Chapter 4 analysis of the experimental

results are presented. The reaction kinetics of the switchable adhesive are studied in Chapter 5.

2. THEORETICAL BACKGROUND

2.1 Properties of Polyester Film

The characteristic chemical structure in all polyesters is the ester linkage in the main chain. Polyesters differ significantly from each other by the number of the ester linkages and backbone structure. Polyesters are used in many different ways such as fibers, films, surface coating resins, rubbers and plasticizers. The most common polyesters used in film industry are poly(ethylene terephthalate) (PET) and poly(ethylene naphthalate) (PEN). [1] (p.694)

PET film manufacturing started to grow rapidly on the back of an increasing demand for PET fibres. In 1960, ICI developed the first PET film for food packaging application. The manufacture of PET employs a polycondensation reaction of either the ester interchange of dimethyl terephthalate with monoethylene glycol or the direct esterification of terephthalic acid with monoethlylene glycol. [2]

The unique properties of PET come from the combination of the aromatic terephthalate and the flexible monoethylene glycol. The properties of a standard PET film include high mechanical strength, flexibility, excellent visual properties, flatness and dimensional stability. In addition PET film retains its physical, chemical and electrical properties up to temperature of about 150 °C. [2] PET film is commonly used in electrical applications such as slot liners for motors and as packaging material. [1] (p.719)

Poly(ethylene 2,6-napthalene dicarboxylate) (PEN) is the condensation product of 2,6-naphthalene dicarboxylic acid and ethylene glycol. PEN was first patented by Cook and co-workers in 1948 but it was not until the 1970s that it was commercially manufactured by Teijin Ltd. [3] (p.464); [4] PEN film has high tensile strength, high temperature resistance, high UV resistance and good barrier properties. However, the manufacture of PEN was expensive before the dicarboxylic acid monomer became available in larger quantities. In the 1980s and 1990s PEN was produced by several companies including Shell, 3M, DuPont, Eastman and ICI. [1] (p723)

The difference in structure between PET and PEN is the condensed aromatic rings (the naphthalene group) in PEN where as PET has just single aromatic ring [3] (p.464). The structures of PET and PEN can been seen in Figure 1.

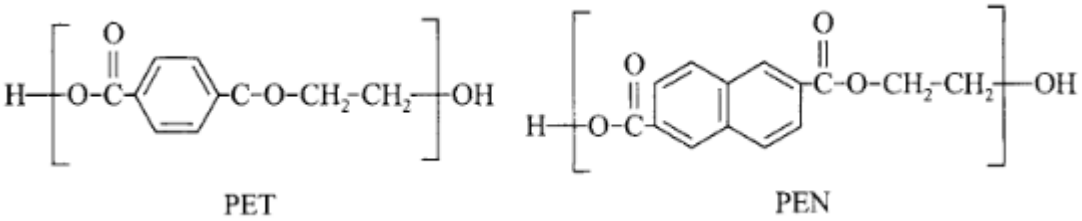

Figure 1. *Structures of PET and PEN [1] (p.723)*

The naphthalene in the backbone gives PEN a stiffer chain that leads to the excellent mechanical and thermal properties and dimensional stability. The glass transition temperature (T_g) of PEN is about 124 °C and the melting temperature (T_m) is circa 270 °C. These are much higher than the values of PET (T_g = 75 °C and T_m = 256–265 °C). [1] (p.723) PET and PEN film also have similarities. Both are transparent to visible light but the mechanical properties of PEN film are more stable when it is exposed to UV light or γ-irradiation than mechanical properties of PET. [3] (p.464)

2.2 Manufacturing of Polyester Film

Polyester film is manufactured using a biaxial orientation technology which was developed in the 1960s. In this technique, the film is first stretched in one direction and then stretched again in a second, perpendicular direction. This increases the film's mechanical properties and lowers its gas permeability. [16] The process involves separate stretching stages where the original amorphous film is passed over heated rollers and then fed to the stenter oven. When film passes over the rolls it is drawn in the machine direction (MD) and in the stenter oven the film is drawn in the transverse direction (TD). The film manufacturing process is shown in Figure 2. [4]

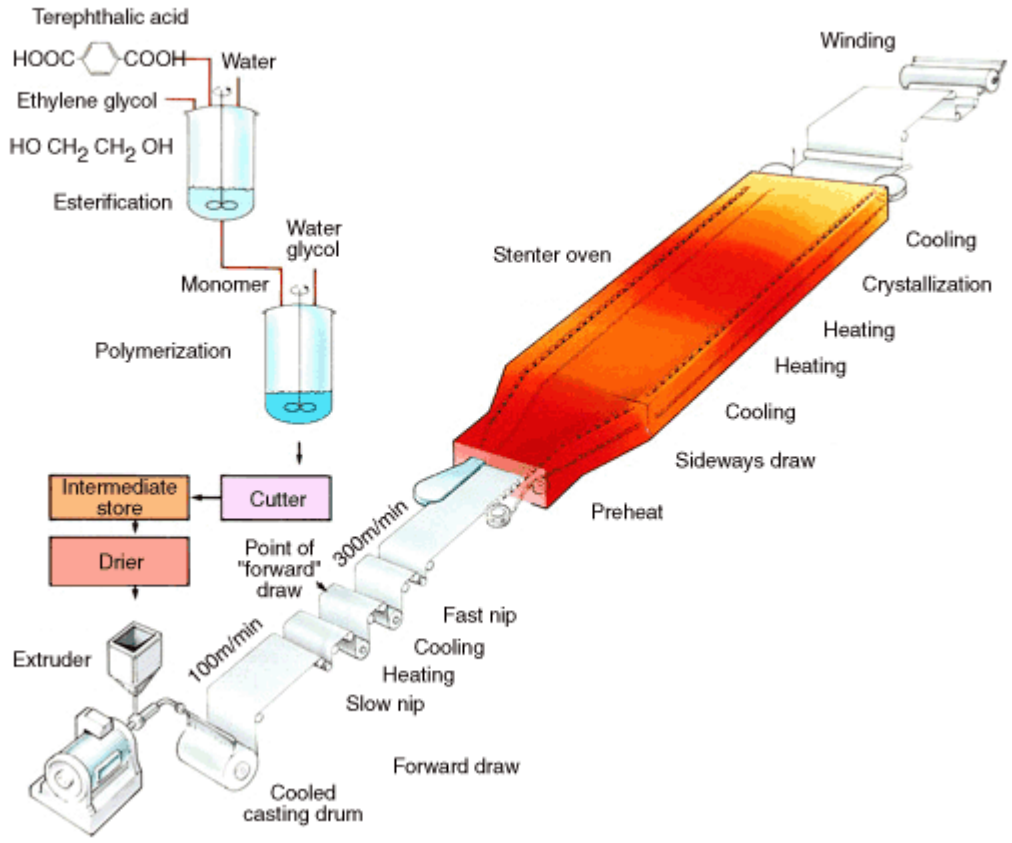

Figure 2. *Process flow of poly(ethylene terephthalate)(PET) film [5]*

With this manufacturing process the thickness of finished film can be controlled between 0.6 µm and 350 µm. The film making process, from polymer granulates to final product can be divided into four stages: polymer preparation and handling, extrusion and casting, drawing and heat setting as well as slitting, winding, and recovery. [4]

Polymer Preparation and Handling

The polymer granulates or chips are fed to the casting stage by a mechanical extruder or the polymer can be fed directly as a melt from a continuous polymeriser. If a single screw extrusion process is being utilized the polymer granulates must first be dried. Drying of granulates is essential because the polyesters are hydrophilic and water in granulates can cause hydrolysis of the polymer chains leading to a reduction in the molecular weight. The drying is carried out at about 180 °C and granulates are kept in the oven for several hours. In the twin screw extrusion process the moisture is removed by the application of vacuum. [4]

Extrusion and Casting

After the blending and drying the polymer is melted and extruded through a slot die to generate a uniformly thick melt curtain. The polymer is filtered before passing through the die to remove residues and degraded polymer from the extrusion process. The output of a commercial extruder is usually about 2 to 3 tonnes per hour, but outputs up to 3.5 tonnes per hour can be used for the production of thicker films. The thickness of the film is measured constantly and a thickness profile is formed based on the measurements. The profile is used to adjust the flow across the die and maintain a constant thickness for the film. [4]

Casting of the film creates a continuous and uniformly thick film of solid, noncrystalline polymer. In the casting process the polymer film, which is still in a melt phase, is deposited onto a cold casting drum. The step is designed minimize crystallization, which if present can cause the film to be brittle and lead to splitting during further processing. The cooling of the film has to happen quickly to below its glass-transition temperature where crystallization ceases. The cooling is achieved using recirculated water of temperature normally between 10 °C to 15 °C in the casting drum. The contact between film and casting drum surfaces is improved by electrostatically charging the film surface. This is achieved using a pinning wire or blade electrode stretched across the drum. [4]

The casting drum is usually polished to avoiding any patterning or contamination of film. The surface of the drum must be hard so it will not be easily damaged in the process. Chrome plating is applied to the drum in order to avoid corrosion. [4]

Drawing and Heat Setting

The film goes from casting through a preheat zone, which includes multiple heated rolls where the film temperature is raised to about 15 °C above its glass transition temperature. This temperature is critical because then the film can be stretched to its final length. The machine direction stretch occurs between two nip roll systems running at different speeds. The purpose of machine direction stretching is to orient the chains in the machine direction, improving the film tensile modulus and strength in machine direction. The film is stretched both in machine direction and transverse direction. [4]

Stretching in the transverse direction happens when the edges of the film are clipped and led along diverging rails. The stretching of PET film happens around 100 °C, while PEN film needs a higher temperature of about 135 °C. The purpose of stretching the film in the transverse direction is to improve the film properties in TD and this occurs by realigning some crystallites originally oriented in the MD, into the transverse direction. [4]

After the drawing processes the film is ‘heat set’. In this process the film goes through three or more regions of stenter oven which are set at elevated temperatures. The temperature of film can reach up to 230 °C during the heat set stage. The purpose of heating is to develop further the crystalline morphology in the film. The crystalline structure keeps the improved mechanical properties in the machine and transverse directions. The crystallinity of the film can raise 30–40 % during the heating stage. [4]

Slitting, Winding, and Recovery

The last stage of processing is slitting and winding the film. The film edges are thicker than the film from the centre so the edges must be cut off in order to enable effective winding. This occurs upon the exit of the stenter oven with the trimmed film edges being recycled back into the extrusion process and the centre portion of the web being wound onto rolls. [4]

Both PET and PEN are inert polymers. The surface of the film can be coated to tailor the surface properties for given application. Coatings are needed when the film has to have specific surface properties such as barrier, release or adhesive characteristics. The coatings can be applied to either one side of the film or both sides. The coatings used for PET and PEN film are mostly acrylic-, vinyl-, polyester- or polyurethane based and they can be formed with either in-line or off-line coating. In-line coating happens just before film enters the stenter and in the case of off-line coating the process involves unwinding and then coating the preformed film. In in-line coating the material used is aqueous-based and in off-line coating the material can be either aqueous or solvent-based coating. [4]

2.3 Applications of PEN Film

PEN can be classified as a high-performance polymer since it meets the high standards of modern mechanical, thermal and electrical engineering. PEN is particularly preferred in electrical and electronic applications and is typically utilized as the base film for high density magnetic recording media [3] (p.464). The excellent heat and barrier properties makes PEN film a good choice for high performance packaging. The use of PEN in packaging material can even replace glass in some packaging applications. [2]

PEN film can be used for electrical insulation applications because of its excellent heat resistance. Other applications where the heat resistance of PEN is needed are for example in flexible warming circuits and battery heaters. PEN is showing potential for container material because of its higher process temperatures and lower permeability to gases. [1] (p.724)

PEN has advantages as a substrate for flexible displays because of its low haze, low coefficient of thermal expansion (CTE), good chemical resistance, low moisture

absorption and low price compared to other suitable materials. On the other hand the upper operating temperature of PEN and its surface roughness are not optimal. The thermal and dimensional stability of PEN can be improved with a heat stabilization process. After the heat stabilization, the operating temperature of PEN film increases to 200 °C. In addition, a surface planarization can generate highly smooth surfaces on PEN film, allowing it to be used in flexible display applications, such as OLED displays. [6] Figure 3 shows the flexible display based on OLED technology.

Figure 3. *Flexible OLED display [7]*

DuPont Teijin Films manufactures PEN film under the brand name Teonex®. It is marketed as a good material choice for demanding flexible display applications, such as high performance touch screens, flexible OLEDs, e-paper, high-barrier flexible substrates, flexible microelectronics and thin film transistors (TFTs). Optical grade Teonex® film that has been heat stabilised is also now commercially available and it can be used for applications that have the most demanding requirements. [8]

Both PET and PEN film are always modified between initial manufacture and final application. This is the role of a converter who will cut, coat or remodel film. In many cases where film is part of a coextruded article, an adhesive layer will be important, so one of several technologies which are key to the polyester film industry is adhesive technology.

2.4 Adhesives

Adhesion is a general term and it is used to refer to the attraction between surfaces. The definition of an adhesive is a material that can join materials together and resist

separation when it is on the surfaces of these materials. [9] (p.1) Adhesion between materials can be described thermodynamically, but this cannot be measured precisely [10] (p.1). An adhesive can mean different materials for example glue, paste and cement. The base materials that an adhesive joins together are referred to as substrates. [9] (p.1)

The science and technology of adhesion and adhesives started only recently in the middle of the 1940s when the technology of synthetic polymers was developed. The reason why synthetic polymers are used as adhesives is that they have properties that make them adhere to other materials. This adhesion is so strong that the forces applied to one substrate are transmitted to another substrate through the adhesive. Adhesives have made it possible for new materials to be developed for demanding technological purposes. The research for new adhesives with a wide range of properties has increased as more synthetic polymers have come to the market. Specific adhesives with very diverse manufacturing and performance requirements are needed nowadays for both industrial and domestic applications.[9] (p.2)

Adhesion properties are affected by the wetting and the tackiness of the surface. The material is defined to be tacky when the energy required to break the surface bonds is a thousand times larger than the simple interfacial energy. In addition, a polymer needs to have the right balance between softness and its energy dissipation capability. The softness is needed to achieve a good contact between two materials and the ability to dissipate energy is needed during the separation process. [11]

2.4.1 Mechanisms of Adhesion

The force of adhesion, which acts on a surface, is dependent on the nature of the adhesion. There are four mechanisms of adhesion which have been recognised. These mechanisms are mechanical interlocking, diffusion theory, electronic theory and adsorption theory. Each theory may be appropriate in different circumstances but the best known theory is the adsorption theory. [9] (p.56)

The mechanical interlocking theory implies that the major source of adhesion is the interlocking of the adhesive into the roughness of the surface on the substrate. With the mechanical interlocking a service life of even ten years can be achieved. This theory does not include smooth surfaces that have good adhesion and therefore it does not have wide applicability. [9] (p.57-59)

The diffusion theory suggests that mutual diffusion of polymer molecules across the interface causes the adhesion of polymers. This theory requires mobility and mutual solubility of the adhesive and substrate. The mutual solubility happens if both adhesive and substrate have similar values of the solubility parameters. This theory is not

applicable when a polymer is highly crosslinked, crystalline or below its glass transition temperature. [9] (p.71-73)

The electronic theory states that the electrostatic forces, caused by different electronic band structures of the adhesive and substrate, affect significantly the intrinsic adhesion. The difference in electronic band structures causes electron transfer which affects the formation of a double layer of electrical charge at the interface. However, wider studies have shown that the electrical double layer does not affect significantly the adhesion forces on the interface. [9] (p. 74-78)

The adsorption theory of adhesion claims that the materials have adhesion because of the interatomic and intermolecular forces. These forces are between the atoms and molecules on the surfaces of adhesive and substrate. The secondary interatomic and intermolecular forces are for example van der Waals forces and hydrogen bonds. Chemical bonding can sometimes occur at the surfaces. [9] (p.78) The adsorption theory, in most cases is regarded as the main mechanism of adhesion but still in certain circumstances any of the four mentioned mechanisms can contribute the intrinsic adhesion. [9] (p.96)

2.4.2 Pressure-sensitive Adhesives

Pressure-sensitive adhesives (PSAs) are adhesives that are permanently tacky. They form immediate adhesion when light pressure is applied and the adhesion process does not need further activation such as treatment with solvents or heat. PSAs were already in use in the late 19^{th} century when they were used in medical tapes and dressings. The first patent of PSAs was published in 1846. Some PSAs can also be easily removed with light force. One of the characteristics of PSAs is that they have strong internal strength so the bond between the adhesive and substrate always breaks first. [10] (p.1–2)

PSAs require an optimum balance of elastic and viscous properties in order to achieve strong adhesion and be able to debond. The PSAs must possess both liquid and solid properties so that it can flow to make conformal contact with a substrate and to achieve wetting when it is being drawn at low strain rates whilst withstanding high shear stress. Also viscoelastic properties are needed to achieve energy dissipation when the adhesive is being drawn at high strains during debonding. [12] The PSAs need to have high shear strength and it cannot leave residues on a substrate after debonding. [10] (p.2)

2.4.3 Switchable Adhesives

Ideally, a switchable adhesive should possess several important characteristics. First, the adhesive should instantaneously switch from tacky to non-tacky. Second, the adhesive should be stable over time when temperature, humidity and illumination are at standard conditions. Third, the adhesive material should be similar to standard adhesives so that

no expensive chemical pretreatments are needed. Last, the adhesive should change its adhesion only when it is at the conditions where the switch is desired. In most applications the ease of debonding between both surfaces is also important. [12]

Adhesives that switch off and on when heat is applied to cause a surface phase transition is especially interesting for medical applications. An example of a temperature switchable adhesive is a liquid crystalline polymer where the surface structure and wettability is changed when temperature changes. The problem with temperature switchable adhesives is that they require specific chemical compositions and molecular architecture in order to work so they cannot be used widely. [12]

DuPont Teijin Films has currently two materials that are prepared and coated onto polyester film and act as temperature switchable adhesives. These adhesives are proprietary products, but the knowledge of their properties and performance is limited. The purpose of this thesis is to study and characterise the properties and the switching behaviour of one of the adhesives. The adhesive studied has been used with PEN film during the fabrication of flexible OLEDs for lighting and displays applications. PEN film is available initially with a coating of the switchable adhesive applied to the film. The OLED structure is fabricated on top of PEN film which is anchored to a rigid glass carrier, using the adhesive. In the final step of fabrication, the OLED is peeled off from the substrate, while the adhesive remains attached to the glass carrier.

2.5 Flexible Displays and OLED Technology

Flexible electronics is currently a large and growing market, whose applications vary from flexible displays to flexible photovoltaic cells and biomedical sensors. [13] Polyesters have many properties that are needed for flexible display applications. For example PEN film has good clarity, low coefficient of thermal expansion, high chemical resistance as well as low moisture absorption. [6]

Flexible displays with OLEDs have already been demonstrated as prototypes. Several prototype designs employ polymer films. The OLEDs in displays have many advantages compared to fluorescent lights and light emitting diodes (LEDs). One advantage is that the contrast of colours and the transition from white to black happens more rapidly. This is useful not only for displays applications but also in commercial light advertising. [13] OLED displays have already been used in rigid displays in technological applications like smart phones and OLED TVs. Because of their thin design, OLEDs can also be built on flexible substrates. [14]

OLEDs for flexible displays demand more strict requirements. Excellent mechanical properties are needed for the film to be suitable for a roll-to-roll fabrication process. Also when the final product is bent there should be no mechanical failure between the organic and inorganic materials. The structure of an OLED display contains multiple

layers such as a flexible polymer substrate, organic–inorganic multi-barrier-layer, brittle transparent inorganic anode, light-emitting layer, TFT layer, metal cathode, and encapsulating layers. The structure of a representative flexible OLED is shown in Figure 4. [6]

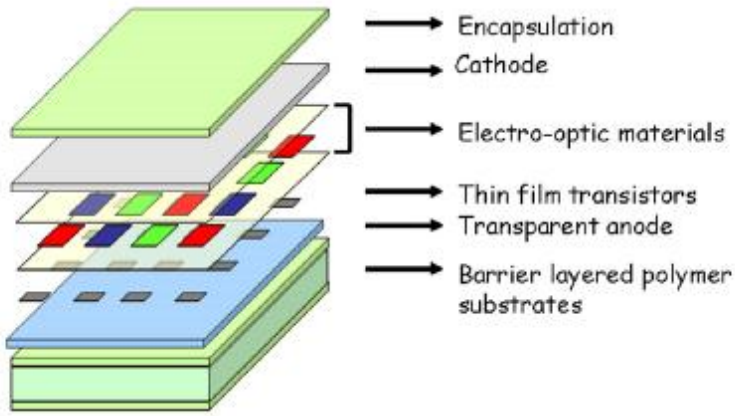

Figure 4. *Cross-sectional structure of flexible display with OLED technology [6]*

The advantage of flexible displays is that they are thinner and lighter than the corresponding rigid displays. In addition they are robust, conformable and they can be rolled in to a small space. The flexible display can be produced in high volumes with a cost effective roll-to-roll processing method which implies the future manufacturing costs of displays will drop significantly. [15]

OLEDs require very specific conditions to operate and the glass substrate used currently provides these conditions very successfully. The limitation of glass is its rigidity and it can be used just in flat panel applications. The flexible substrate replacing glass should have similar properties to glass like its clarity, thermal and dimensional stability, excellent barrier properties, smooth surface and good optical properties. [6] One candidate for a flexible substitute for glass is PEN film due to its mechanical and thermal properties and also its high transmittance. Compared to glass, PEN provides a lower barrier performance to oxygen and water, so PEN film needs multiple organic gas barrier layers in order to function effectively in this application. [14]

A problem with the flexible substrate based OLED technology is the layer alignment when processing the high performance electronics on a flexible substrate. To solve this problem the bond-debond adhesives also called switchable adhesives can be used. The adhesive is used to stick temporarily the flexible substrate on a glass carrier so that the fabrication of the electronics can take place. When the electronics are completed the flexible substrate is peeled away and the adhesive remains bonded to the glass, leaving the flexible substrate clean. [16]

Better materials and also further development is needed to manufacture flexible OLED lighting and displays that are durable. The problem with plastic film is that it needs

barrier layers added to its surface in order to protect the OLEDs from moisture and oxygen ingress. At the moment several companies are researching to develop a flexible OLED for multiple applications like displays and lighting. There are already demonstrations of flexible OLEDs with a commercially available product being expected this decade. [17]

3. RESEARCH MATERIALS AND METHODS

3.1 Materials

The adhesive used in this study was coated on PEN film grade Q83 of thickness 25 µm with application of the coating being performed in clean room to avoid any contamination of the coating. The adhesive was protected with siliconised interleave before it was wound up into a roll. The film with the adhesive coating was cut into strips, 4 cm by 12 cm and then laminated to glass microscope slides. These laminates were produced using a Hirst laminator, set at a temperature of 60 °C, a pressure of 25 psi and a speed of 25.4 cm/min.

The samples were left to cool down to room temperature after the lamination process. The quality of laminate was assessed and only the laminates with no trapped air bubbles, contamination in the coating or those that were fully sealed were accepted for further testing. After lamination the samples made were cured either in an air circulating oven or on hotplate at different times and temperatures depending on the test applied to the laminates. For the surface analyse measurements the laminates were peeled by hand to expose the switched adhesive. The lamination process is presented in Figure 5.

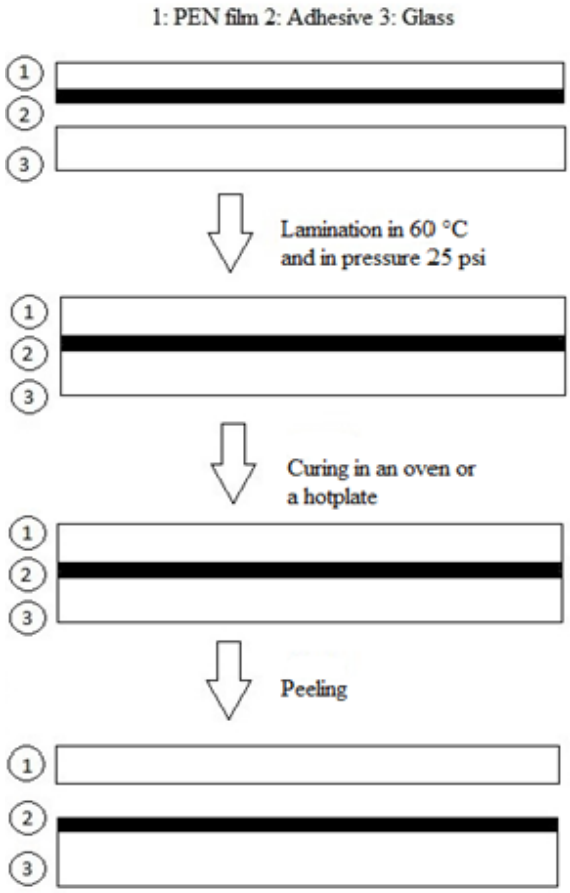

Figure 5. *Lamination process*

The adhesive samples for thermal analysis measurements were made separately to have thicker adhesive layer that can be put to mechanical tests and to have adhesive sample without PEN film to analyse with differential scanning calorimeter (DSC). The solution of adhesive was made using the same recipe as previously when the adhesive was coated on the film in a clean room. The non-cured adhesive was cast onto circular aluminium trays with diameter about 5 cm. The casting was performed by dropping a small amount of solution from a pipette onto an aluminium tray that was covered with silicon film. This prevented the adhesive sticking to the tray. After casting the samples were left in a fume cupboard overnight to cure and dry. To remove solvent residues from the adhesive, the samples were placed in a vacuum oven, overnight at a temperature of 40 °C.

3.2 Surface Energy

The surface free energy is a measure of how much work is required to form a new surface when separating two phases. When the adsorption on the surface of a solid is zero the surface free energy and the surface tension of the solid are equal. [18] The surface tension measures the intermolecular forces on the surfaces. The tension is caused by the attraction of two surfaces which results in a loss of a number of molecules

in the surface region. When the amount of molecules decreases the intermolecular distance increases and this requires work to be done. When the system returns its normal configuration the work is returned and this explains the tension in surfaces and surface free energy. [9] (p. 18)

Several different approaches can be used to evaluate the surface free energy of solid materials. All of these approaches use a measurement of the contact angle for different liquids dropped on a sample surface. [19] The angle measured is the angle, θ that liquid drop forms with the solid surface [20]. The results of calculated surface free energies however depend on a chosen method. The Young equation (eq. 1) is used in describing the liquid drop equilibrium

$$\gamma_{SV} = \gamma_{SL} + \gamma_{LV}\cos\theta \quad (1)$$

where γ_{SV} is the surface energy of the solid, γ_{SL} is the interfacial tension between the solid and the liquid, γ_{LV} is the surface tension between the liquid and vapour phase and θ is the contact angle on a solid surface. Figure 6 shows the liquid drop and a measured contact angle. However, in the equation there are two unknowns, the solid surface free energy and the interface free energy between the liquid and the solid, so several theories continuing from Young's equations has been developed. [19]

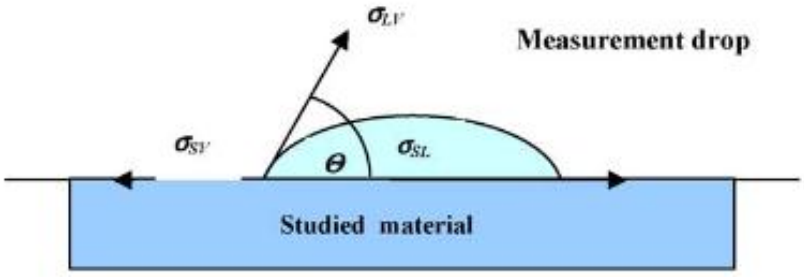

Figure 6. *Graphical presentation of the Young's equation [18]*

Different methods to evaluate the surface free energy of polymers have been investigated in literature, namely the harmonic mean equation, the geometric mean equation, and Neumann's equation [19]. The method used in this study is the harmonic mean equation, because it is recommended for use on lower surface energy surfaces such as polymers [21].

The intermolecular energy between two materials results from the summation of a dispersion component and a polar component. Since the surface tension is proportional to the intermolecular energy, the surface tension γ itself is a sum of a dispersion component γ^d and a polar component γ^p. The interfacial tension between a liquid and a solid polymer can then be evaluated by the harmonic mean equation as follows

$$\gamma_{SL} = \gamma_{SV} + \gamma_{LV} - 4\left(\frac{\gamma_{LV}^{d}\gamma_{SV}^{d}}{\gamma_{LV}^{d}+\gamma_{SV}^{d}} + \frac{\gamma_{LV}^{p}\gamma_{SV}^{p}}{\gamma_{LV}^{p}+\gamma_{SV}^{p}}\right) \quad (2)$$

where γ_{SV}^{d} and γ_{SV}^{p} are the dispersion and polar components of the surface energy of the solid, and γ_{LV}^{d} and γ_{LV}^{p} are the dispersion and polar components of the surface tension of the liquid. [20]

By substituting Young's equation into the harmonic equation above, the following can be obtained

$$\gamma_L(1 + cos\theta) = 4\left(\frac{\gamma_{LV}^{d}\gamma_{SV}^{d}}{\gamma_{LV}^{d}+\gamma_{SV}^{d}} + \frac{\gamma_{LV}^{p}\gamma_{SV}^{p}}{\gamma_{LV}^{p}+\gamma_{SV}^{p}}\right) \quad (3)$$

If the contact angles of two liquids with known γ^d and γ^p are measured, it is possible to solve equation (3) simultaneously and calculate the γ_{SV}^{d} and γ_{SV}^{p} for the solid. [20]

3.2.1 Wetting

The adhesive properties are affected by wetting and that is why the control of wetting properties is important. Wetting is defined by how well the liquid is spread on the surface as a continuous film. A number of different surface treatments to modify the surface can be applied in order to control its wettability. The molecular organization of the surface controls the interfacial energy which affects the wettability on hard substrates but on a deformable substrate the wetting is governed by viscoelastic dissipation in the material. [11]

Wetting can be measured when a liquid drop is resting on a solid substrate like in surface free energy measurements. The system forms a three-phase contact, see Figure 6 where a force balance at the interface provides a relationship between the tension forces and the contact angle, as defined by the Young's equation showed before in equation (1). The term γ_{SV} in Young's equation represents the surface free energy of the substrate that is affected by vapour from the liquid. This surface free energy value can be remarkably lower than if the substrate was in vacuo γ_S. The following equation defines the reduction in surface free energy

$$\gamma_{SV} = \gamma_S - \pi_S \quad (4)$$

where π_S is the spreading pressure of the adsorbing vapour. For the spontaneous wetting could be occurred, the following equations must be true

$$\gamma_{SV} \geq \gamma_{SL} + \gamma_{LV} \quad (5)$$

$$\gamma_S \geq \gamma_{SL} + \gamma_{LV} + \pi_S \quad (6)$$

When the wetting to the solid happens completely the angle of the liquid drop, θ is 0°. [9] (p.19-20)

3.2.2 Work of Adhesion

The work of adhesion, W_{AB}, is closely related to the wetting of solids by adhesives and it measures the work required to separate a unit area of two interfaces where secondary forces are acting. Work of adhesion is related to the surface energies by the Dupre's equation [9] (p.82). To calculate values for work of adhesion, the surface energy must be calculated first from the contact angle measurements.

In Dupre's work in 1869 the work of adhesion between two liquids in contact is expressed as

$$W_{AB} = \gamma_A + \gamma_B - \gamma_{AB} \tag{7}$$

where the A and B designate the two condensed phases. Combining the equation (7) and the Young's equation (1), the Young-Dupre equation is formed

$$W_{AB} = \gamma_L(1 + \cos\theta) \tag{8}$$

where γ_L is the surface tension of the liquid and if A is the solid, θ is the contact angle of B on A. [22]

The estimate for work of adhesion is given in an equation below [21].

$$W_{AB} = 4\left(\frac{\gamma_{LV}^d \gamma_{SV}^d}{\gamma_{LV}^d + \gamma_{SV}^d} + \frac{\gamma_{LV}^p \gamma_{SV}^p}{\gamma_{LV}^p + \gamma_{SV}^p}\right) \tag{9}$$

The values of the surface energy components of both the substrate and the adhesive should be as large as possible in order to maximize the work of adhesion [9] (p.82).

The contact angles were measured with a VCA 2500 XE Goniometer. The surface free energy of a film surface can be obtained by measuring the contact angle of two pure liquids. The liquids used in these measurements were purified water and diiodomethane. Diiodomethane is used as it has no polar component contributing to its overall surface tension. However, in the literature there are inconsistencies with some authors reporting diiodomethane polar component value of 2.3 dynes/cm. The accepted values for surface tension of water and diiodomethane are shown in the Table 1. [23] For the measurements 4 µl droplet of water and 2 µl droplet of diiodomethane were utilised, with the droplet size being chosen as a result of the camera field of view limitation. For every sample the contact angle of both liquids were measured five times and the dispersive and polar components were calculated from the average value.

Table 1. *Surface tension of water and diiodomethane [23]*

Liquid	Polar component (dynes/cm)	Dispersive component (dynes/cm)	Surface Tension (dynes/cm)
Water	51.0	21.8	72.8
Diiodomethane	0	50.8	50.8

In this study the surfaces measured were a microscope glass slide and both sides of 25 µm thick PEN film which was coated on one surface with adhesive. The glass slide was tested initially and then after laminating it with adhesive coated PEN film, curing it at 180 °C and peeling the PEN film off. The second measurement performed at the glass slide was in fact a test of the residual adhesive. In addition, both sides of the PEN film were tested after laminating, curing and peeling. Also, measurements were performed on PEN film without adhesive. Each sample was measured five times and the average value was calculated.

Measurements were also performed on the adhesive coated onto PEN film which has been laminated on the glass slides and cured at different temperatures on a hotplate for two minutes. The curing temperature range was from 50 °C to 200 °C. The PEN film was peeled off after the curing and the contact angles for both surfaces, which were created by peeling at the interface, were measured. After the PEN film was peeled from the glass slide and the adhesive found to have switched to the glass slide when the curing temperature had been higher than 80 °C. The adhesive on glass slide samples were labelled according to curing temperature to AG80, AG90 and so on.

To study the behaviour of the adhesive after exposure to different temperatures the adhesive on the PEN film was cured in the oven for two minutes at temperatures 50 °C, 60 °C, 70 °C, 80 °C, 90 °C, 100 °C, 120 °C, 140 °C, 160 °C, 180 °C and 200 °C. These samples were labelled according to the curing temperature to AP50, AP60 and so on. The surface energy was measured after the adhesive was cooled back to room temperature.

3.3 Fourier Transform Infrared Spectroscopy

The infrared (IR) spectroscopy measures the absorption of infrared light which is going through a sample. The radiation of infrared light can either be absorbed or transmitted and this depends on the frequency of an infrared beam and the molecular structure of the measured sample. The IR radiation is absorbed and causes vibration to the molecules in the sample at certain wavelengths where the frequencies corresponding to the molecular mode of vibration of the corresponding molecule or chemical group are matched. The IR spectroscopy is used in identification of materials and molecular

structures because functional groups absorb IR radiation at certain characteristic frequencies. [24]

IR radiation in the electromagnetic spectrum appears between the visible light (higher frequencies) and microwave radiation (lower frequencies). The electromagnetic spectrum is shown in Figure 7. The wavelengths of IR radiation are between 0.78 and 1000 µm but most molecules absorb mainly in the mid-IR frequencies which are between 2.5 and 25 µm. IR absorption can also be presented in wavenumbers (n) instead of wavelengths (λ). The definition of wavenumber is the number of waves per unit length while wavelength is defined as the length of one complete wave cycle and is usually expressed in the unit of micrometers (µm). [24]

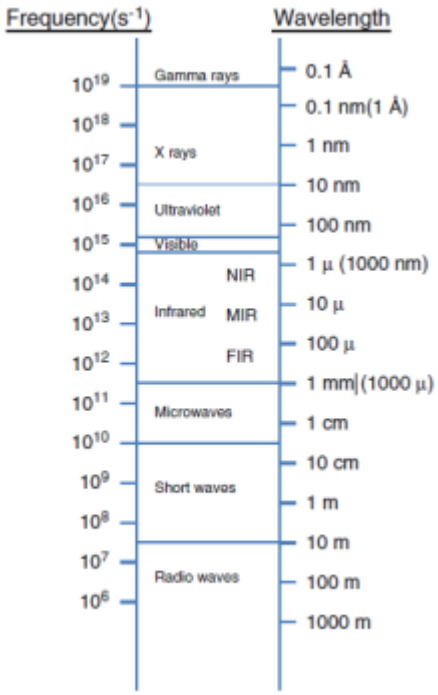

Figure 7. *The electromagnetic spectrum. IR infrared, FIR far infrared, MIR mid infrared, NIR near infrared [24]*

IR radiation causes the chemical bonds in a sample to vibrate and this vibration is different depending on the nature of the bond. These vibrations can be divided into stretching and bending. The stretching can be further divided to symmetric and asymmetric stretching and the bending can be divided to scissoring, rocking, wagging, and twisting. The Figure 8 shows few stretching and bending motions of water molecule. [24]

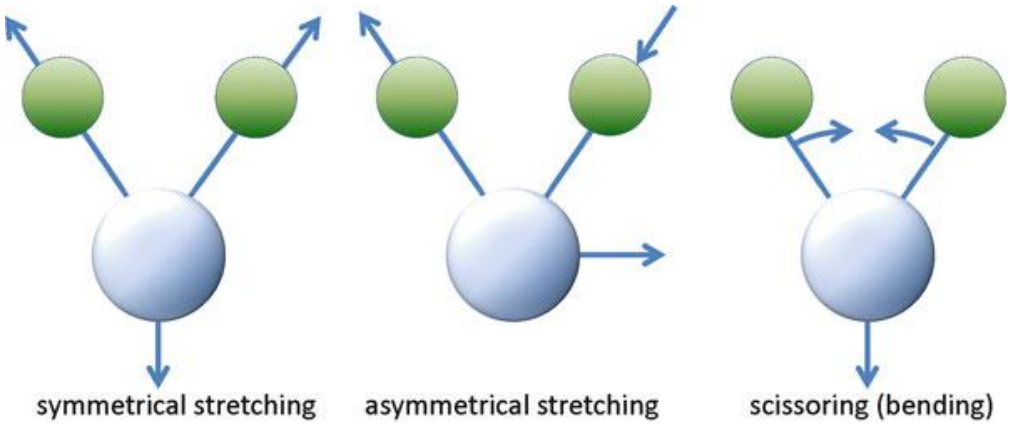

Figure 8. *Stretching and bending vibrational motions for H_2O [24]*

The first Fourier transform infrared (FTIR) spectrometers were available commercially in the 1960s but they were not used widely until recently because of the high cost of equipment. The FTIR apparatus main components include the radiation source, the interferometer and the detector. The Figure 9 shows the basic components of FTIR. The purpose of the interferometer is to split the IR beam into two beams. The one beam strikes a fixed mirror and the other to a movable mirror. The beams are forming interference pattern after they have recombined and IR spectral information is formed when the beam has gone through the sample. The detector measures the interference signal produced. [24]

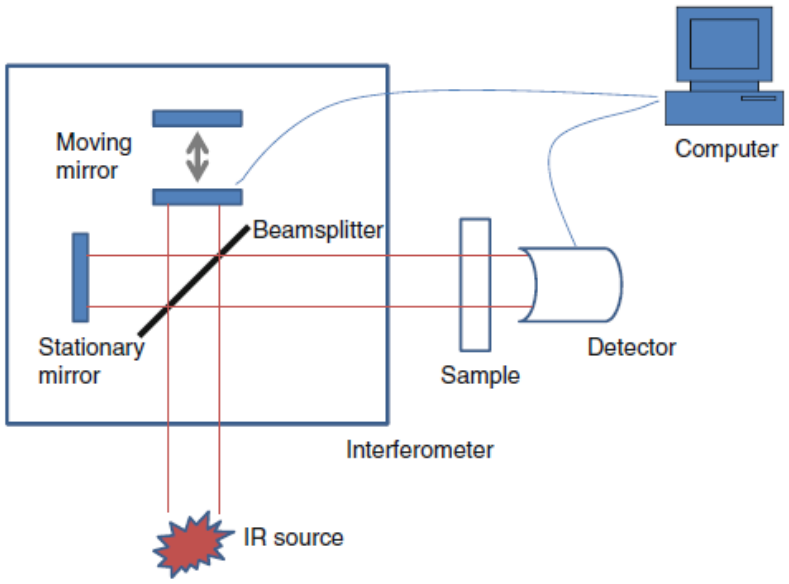

Figure 9. *Modern FTIR system including the light source, the detector and a Michelson interferometer consisting of a beamsplitter, a fixed mirror, and a moving mirror [24]*

The signal collected by the detector is analysed using a computer. The computer reads the information in digital form and transforms the signal into Fourier form. Using Fourier transform the function can be transformed from time domain to frequency

domain. The final IR spectrum can be displayed and interrogated interactively using the computer and display. [24]

In this work the samples were measured with the attenuated total reflectance (ATR) FTIR which is a surface layer technique where the absorbance is measured in direct contact with the ATR surface [25]. The Figure 10 shows how the IR beam travels through the ATR crystal. In the ATR approach the samples do not need further preparation. The sample is put in close contact with an ATR crystal which has high refractive index. When the IR beam is reflected from the internal surface of the ATR crystal, it creates an evanescent wave. This wave extends beyond the crystal surface and projects into the sample. Some of the evanescent waves are absorbed and some reflected and the reflected radiation is ultimately recorded by the detector. [24]

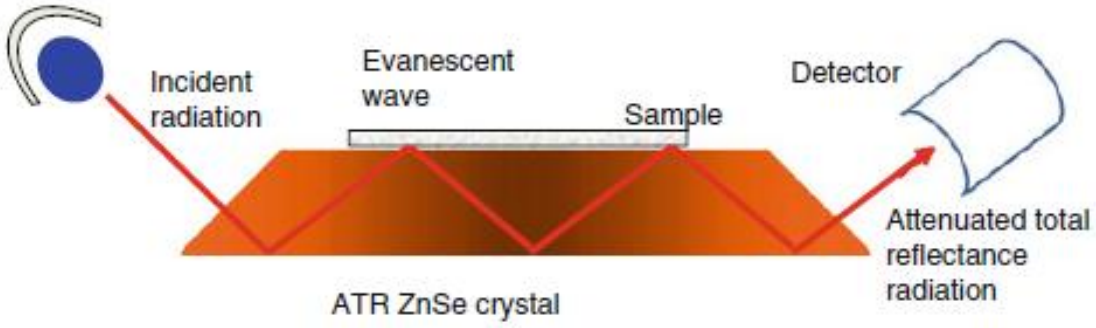

Figure 10. *Attenuated total reflectance (ATR) FT-IR [26]*

A FTIR spectrometer, Thermo Scientific Nicolet, model iS50 was used to collect the IR spectra in the absorbance mode. The sample compartment ATR iS50 was used for these studies. The ATR crystal material is all-reflective diamond and the beam splitter material is potassium bromide. The number of spectra that were collected and averaged of each sample was 32. The resolution of spectra was set to 4.000 cm^{-1} and the laser frequency was 15798.3 cm^{-1}. The wavenumber range of the spectra was from 400 to 4000 cm^{-1}. Wavenumber precision is better than 0.01 cm^{-1}. The FTIR software OMNIC was used to analyse the spectra of the samples.

Two sets of samples were examined using FTIR spectroscopy. In the first case, the samples tested were PEN film coated with the adhesive. These samples were annealed in an oven for two minutes at temperatures 50 °C, 60 °C, 70 °C, 80 °C, 90 °C, 100 °C, 120 °C, 140 °C, 160 °C, 180 °C and 200 °C. The samples are the same than surface energy samples and they are labelled according to the curing temperature to AP50, AP60 and so on. The second set of samples were the laminates cured on a hotplate for two minutes in temperatures 80 °C, 90 °C, 100 °C, 120 °C, 140 °C, 160 °C, 180 °C, 200 °C and 220 °C. These samples were also labelled according to curing temperature to AG80, AG90 and so on like the surface energy samples before.

3.4 Peel Test

3.4.1 Peel Test for Laminates

The peel test used was a 90 degree peel test. The schematic of the testing can be seen in Figure 11. A 90 degree peel test can be used when the other layer of laminate is much more rigid than the layer being detached and it can be performed with a horizontal floating roller fixture. With this fixture the peeled layer can be pulled vertically and the substrate can move freely in horizontal direction. This ensures that the 90 degree angle is maintained through the duration of the test.

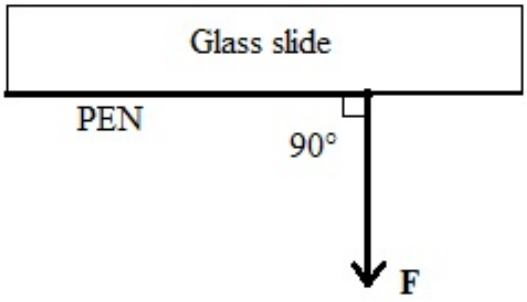

Figure 11. *Schematic figure of 90 degree peel test*

Assuming the adhesive and substrate are linear-elastic materials, when the flexible film is peeled away from the rigid substrate with the adhesive present, the peeling causes a static stress distribution at the interface. In many cases the adhesive does not peel evenly because the adhesive forms filaments across the peel interface and they undergo stick and slip peeling. This behaviour can significantly affect the measured peel force per unit length. [9] (p.239-241)

The material properties that can affect the peel test results are the thickness of the substrate and that of the adhesive. The test method should be selected carefully according to the samples being analysed because the peel test results depend on the variables of the test method. Such variables are the rate of testing, the geometrical arrangement in the test, the temperature during testing, the composition of the surrounding medium and the method of sample preparation. Usually, the rheological properties of the substrate or the adhesive change when the variables of the test method are changed. Also, the interfacial bond strength can differ with variation in the magnitude of the test parameters. [27]

Before peeling laminates, the quality of laminates was checked and the laminates with bubbles were analysed using the image analysis program ImageJ in order to calculate the area fraction occupied by the bubbles. The tests were carried out using an Instron universal testing machine model 4301. The Instron was set up with a standard jaw at its base and a floating roller fixture at the moving crosshead. The crosshead speed was 254

mm/min. The initial peel of the sample laminate was made by hand by peeling the film carefully off the glass. The glass microscope slide was laid horizontally across the floating roller and the loose end of the film placed through the two rollers of the peel tester and into the bottom jaw which was clamped in place.

Three sets of the laminate samples were prepared for peel testing. The first set of laminates were placed on a hotplate at temperatures 80 °C, 90 °C, 100 °C, 120 °C, 140 °C, 160 °C, 180 °C and 200 °C for 2 minutes before testing the peel strength. The measurements were made at room temperature. Eight samples were tested for each temperature and the average of the samples peel strength was calculated.

The second set of laminate samples were cured in the oven instead of hotplate. The samples were kept in a circulating air oven for 20 minutes, 1 hour and 2 hours at temperatures 120 °C, 140 °C, 160 °C, 180 °C and 200 °C. To see the change in peel strength more accurately a third set of samples were cured in an oven from 10 to 60 minutes at 10 minute increments for temperatures of 120 °C, 140 °C, 150 °C, 160 °C, 170 °C and 180 °C. Five samples were tested at each time and temperature value, with the average results being calculated.

3.4.2 Peel Test for Adhesive Cured at Low Temperatures

The peel strength without lamination was also measured to study the adhesion between the PEN film and adhesive when lower curing temperatures are used. The test method was to use epoxy glue to stick another film, PEN Q51 DW, on the adhesive and peel the sample laminate after curing from the PEN film- adhesive interface. The epoxy glue which was employed was commercially available under the trade name Evo-Stik supplied by Bostik. The 25 μm thick PEN film Q83 with adhesive coating was cut to strips of 25 mm by 300 mm. The PEN film Q51 DW which has coating on both sides was cut to same size strips and the epoxy glue was mixed and spread on the other side of PEN Q51 DW film strips. The film strips with epoxy glue were put against the PEN film strips with adhesive coating and the air bubbles and extra glue were pressed away. After the epoxy glue was cured, the samples were placed in an oven for 2 minutes at temperatures 40 °C, 60 °C, 80 °C, 100 °C and 120 °C. The process of making samples is shown in Figure 12.

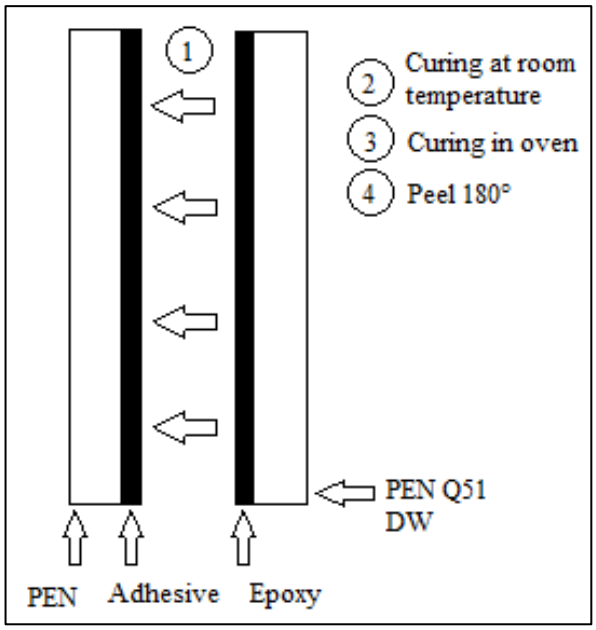

Figure 12. *Samples made for 180 degree peel test*

The peel test method used was 180 degree peel. The 180 degree peel test is used with these samples because both substrates are flexible so using 90 degree peel angle is not possible. The tests were carried out using an Instron universal testing machine model 4301 in room temperature. The Instron was set up with a standard jaw at both ends and the crosshead speed was 254 mm/min. The initial peel from the PEN film and the adhesive interface was made before placing the sample to testing machine.

3.5 Thermal Analysis

3.5.1 Differential Scanning Calorimetry

Differential scanning calorimetry (DSC) measures the heat absorbed or released by a material that is going through a physical or chemical change. The change in a material causes a change in its internal energy and at constant pressure the internal energy is the enthalpy (H). The enthalpy increases when the sample is going through an endothermic process like melting, evaporation or a glass transition. In exothermic reactions the enthalpy decreases. Exothermic processes are crystallization, progressive curing and decomposition. [28] (p.1)

The calorimeter measures the difference between heat flux Q and baseline, which represents the state where no change happens. The enthalpy can be calculated when the heat flux is known. The energy needed to raise the temperature by 1 °C of each 1 g of sample, is called the specific heat capacity (at constant pressure), c_p. The relation of heat flux and heat capacity can be written in equation

$$\frac{Q}{m} = vc_p \tag{10}$$

where v is the heating rate and m is the mass of the sample. [28] (p.1-2)

There are two different designs of DSC, the heat-flux DCS and the power-compensation DSC. In heat-flux DSC the sample and the reference material are heated and cooled together with the temperature program. The temperature of both is measured constantly and the difference between the temperatures of sample and reference material is recorded. The change in temperature (ΔT) is the change in heat flux ΔQ. In power-compensation DSC the sample and reference are under different temperature programs. If changes happen in the sample, the DSC applies power to keep the sample in the same temperature than the reference. The measured difference in thermal power ΔP is related to the change in heat flux ΔQ. [28] (p.2-3)

The glass transition temperature is when the polymer changes from glassy to elastic and rubber-like state. This occurs because the chains segments can move more freely above the glass transition temperature. The glass transition temperature is dependent on the morphology of the polymer. Because morphology of polymer is affected by thermal history and previous processing of the polymer, the sample has to be heated twice to erase the thermal history of a sample. The change in polymer from glassy to elastic can be seen with DSC as a specific heat capacity change. The glass transition temperature is measured as the point when half of the specific heat capacity c_p change has occurred. [28] (p.7)

In this study the first DSC measurements were conducted with PerkinElmer 6000 equipment in an inert nitrogen atmosphere which was calibrated against indium reference and the method used was a heat flux method. To get comparable data from results, each sample measured was weight to be between 5.6 mg and 6.6 mg and the same pan size was used with all the samples. The first samples measured were first heated from -20 °C to temperatures 120 °C, 130 °C, 140 °C, 150 °C and 170 °C with a heating rate of 20 °C/min to evaluate the change in the adhesive after heating. For each temperature the samples were kept at final temperature between 5 min to 2 hours. After the first heating the samples were cooled back to -20 °C with the cooling rate of 50 °C/min but with the samples cures for 2 hours the heating rate used was 20 °C/min so that the samples have enough time to cool to -20 °C. The second heat performed was to 200 °C with the heating rate of 20 °C/min and the heat flux over temperature was evaluated.

The goal of the second part of testing was to evaluate the glass transition temperature of the adhesive. The DSC measurements were made with the PerkinElmer 8500 equipment so that the sample can be cooled to temperature low enough to see the glass transition temperature. The measurements were performed again in an inert nitrogen atmosphere. The heat program was to first cool the sample to -80 °C and kept it there for 5 minutes.

The first heat was conducted from -80 °C to 200 °C and the heating rate used was 20 °C/min. After the first heating the sample was ballistic cooled back to -80 °C. Again the sample was kept at -80 °C for 5 minutes in to ensure the sample has enough time to cool. The second heating was conducted again to 200 °C with the heating rate 20 °C/min. All the scans were analysed using the PerkinElmer Pyris Manager software.

3.5.2 Thermomechanical Analysis

Thermomechanical analysis (TMA) measures the change in sample dimensions as a function of temperature. The changes in dimensions of a sample are caused by changes in the free volume of a polymer. [29]. The expansion can be used to determine the coefficient of linear thermal expansion, α as a function of time. In TMA the specimen is under a constant, but usually small, load. [28] (p.172)

In TMA a small cylindrical shape sample is subjected to a small load using a quartz glass probe which moves in a vertical direction. The position of the probe changes according to the measured sample and the change is related to the coefficient of expansion or glass transition temperature. The probe for measuring the glass transition temperature is a penetration probe with a small contact area. [28] (p.174-176) The glass transition temperature can be determined based on the measured change in free volume as can be seen from Figure 13.

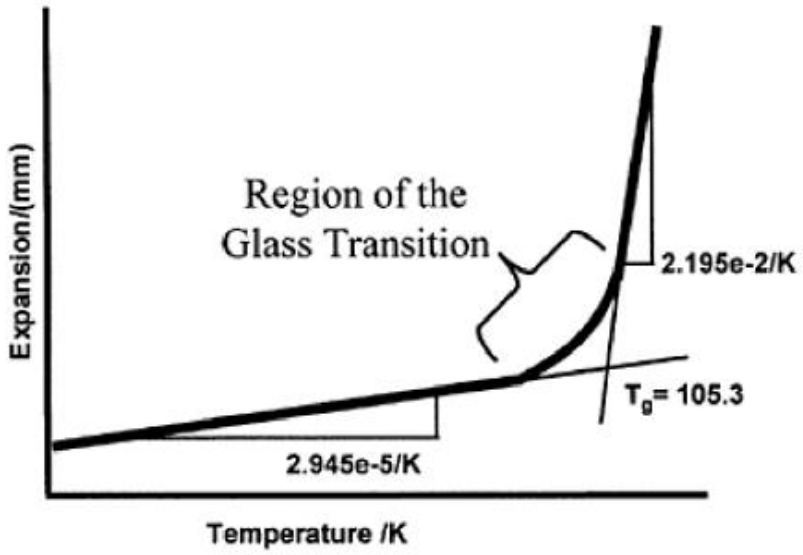

Figure 13. *The T_g can be determined from the tangents of the curve [29]*

TMA measurements were conducted with the Perkin Elmer TMA 7 equipment provided by Intertek MSG Ltd. The sample was cooled to temperature -150 °C using liquid nitrogen and the testing probe used was a 1 mm diameter silver steel penetration probe. The sample was placed in a Perkin Elmer DSC pan with an outer diameter of 6.7 mm. The pan and sample were placed in the Perkin Elmer equipment and the sample was

cooled to the start temperature -150 °C. The force of 150 mN was applied to the sample after it reached the start temperature and the height of the sample was measured and then zeroed.

In the first measurement the sample was heated to 160 °C at a rate of 5 °C/minute under a 150 mN force and the position of the probe was measured over the temperature change. The probe was removed and cleaned before being placed over another region of the sample to perform the second measurement. The sample was cooled back to -150 °C and then the second heating was conducted.

4. RESULTS AND ANALYSIS

4.1 Surface Energy

The surface energy measured in first set of samples was of the surfaces from laminates after peeling an interface and laminate components before peeling (surfaces described in Chapter 3.2.2). The average values of samples were calculated and the results are shown in the Table 2 below. The results were also plotted to graph to illustrate better which samples have similar surface energies as seen in Figure 14.

Table 2. *Average values of surface energies*

Sample	Polar component (Dynes/cm)	Dispersive component (Dynes/cm)	Total surface energy (Dynes/cm)
Glass slide	42.17	26.83	68.98
Adhesive coating on PEN film	19.86	29.44	49.30
PEN film uncoated surface	7.74	38.56	46.30
Adhesive transferred to glass after curing at 180 °C and peeling	48.65	22.80	71.71
Exposed surface of PEN after curing at 180°C and peeling	16.06	36.81	54.62
PEN film uncoated surface, after curing at 180°C and peeling	7.53	36.08	43.61
PEN without adhesive coating	5.52	40.21	45.73

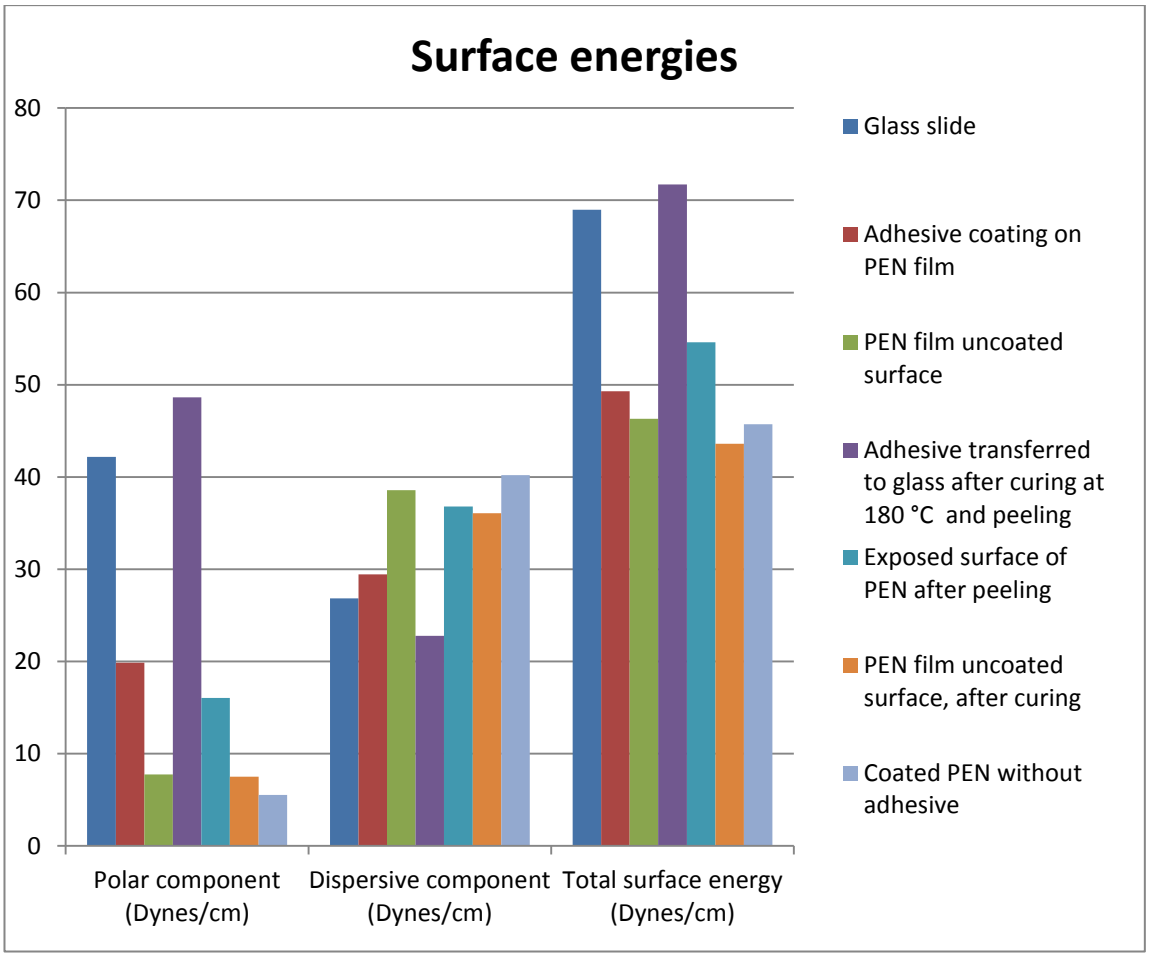

Figure 14. *Graph from surface energy values*

From the results it can be concluded that the surface energy of the adhesive changes after lamination and annealing at 180 °C, when it is seen to switch sides. The total surface energy of the adhesive is closer to that of PEN film before curing and after curing at 180 °C the surface energy of adhesive is closer to glass.

In a further study (AG set of samples and PEN film described in Chapter 3.2.2) the change in surface energy with temperature was examined. Laminates were cured at various temperatures and surface energy of the adhesive measured. The surface energy of the adhesive, which transferred to and remained on the glass surface after peeling and the surface energy of the PEN film interface after peeling are presented in the Figure 15.

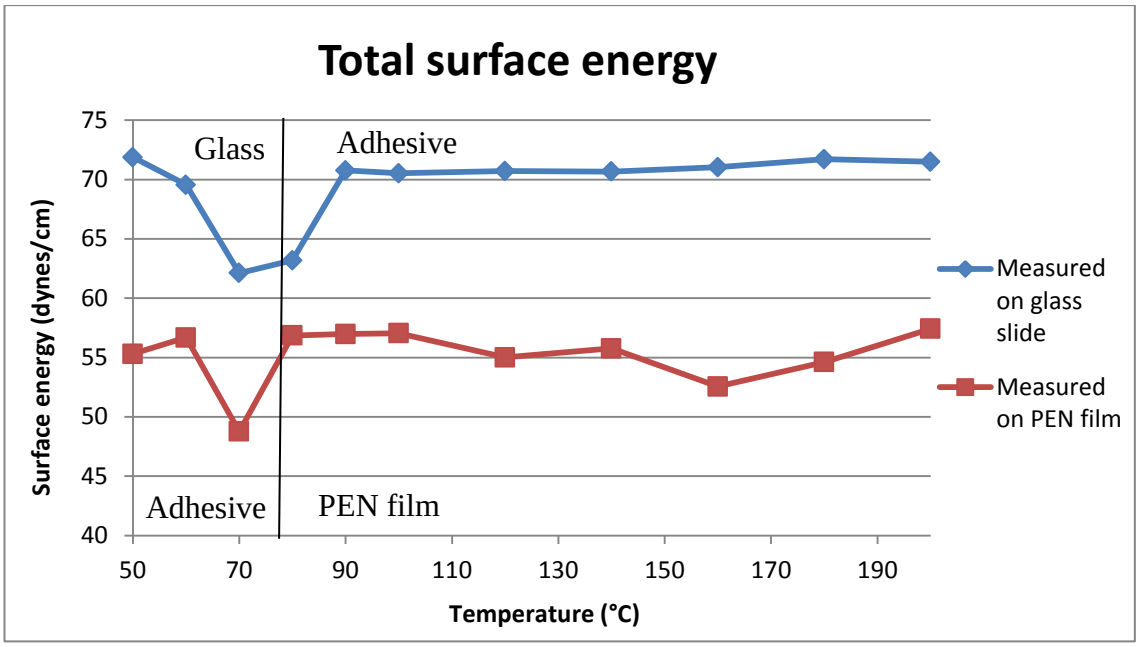

Figure 15. *Total surface energies of the glass slide and PEN film after peeling*

With close examination the adhesive was observed to switch sides after the curing temperature rose 80 °C. The adhesive after peeling remained on the PEN film up to 70 °C and at 80 °C the adhesive had transferred to the glass slide. Figure 16 attempts to illustrate this effect where the surface energy of the adhesive cured up to 70 °C is depicted by the red curve. For curing at above 80 °C the surface energy of the adhesive is represented by the blue curve. Clearly the surface energy of the adhesive changes radically around 80 °C.

An explanation for the low surface energy measured on glass slide below 80 °C would be partial transfer of the unchanged adhesive, whose initial energy is around 50 dynes/cm. The surface energy of partially transferred adhesive is between the surface energy of adhesive before curing (~50 dynes/cm) and the surface energy of glass slide (~70 dynes/cm).

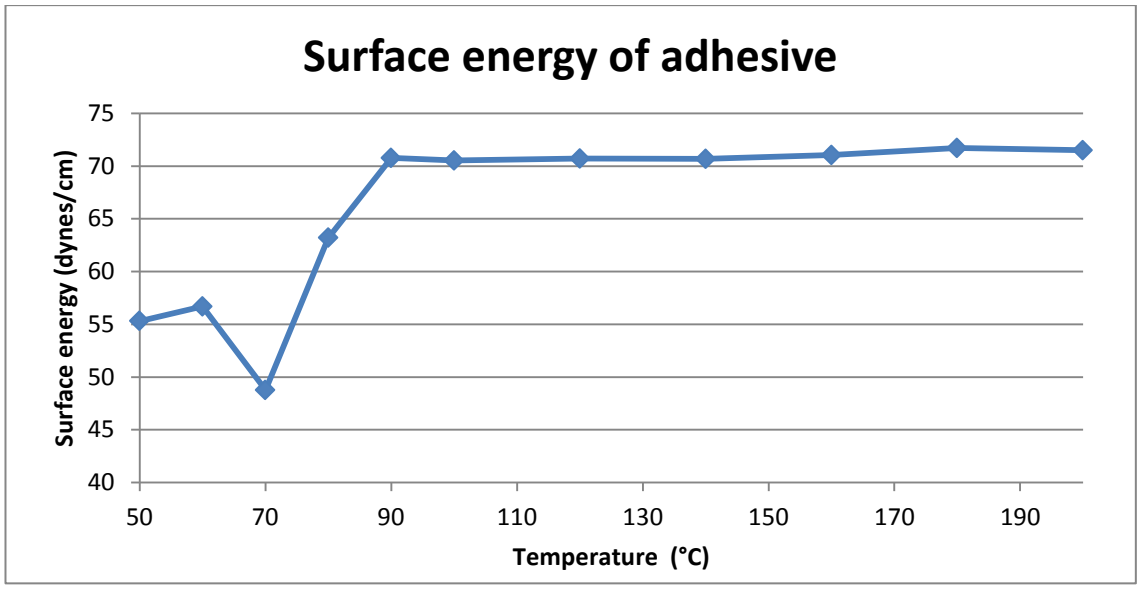

Figure 16. *Total surface energy of adhesive*

The surface energies were also measured of the AP set of samples (described in Chapter 3.2.2), which were cured at different temperatures. The polar and dispersive components were plotted separately to examine if the components change differently when the curing temperature increases. The results are presented in the Figure 17.

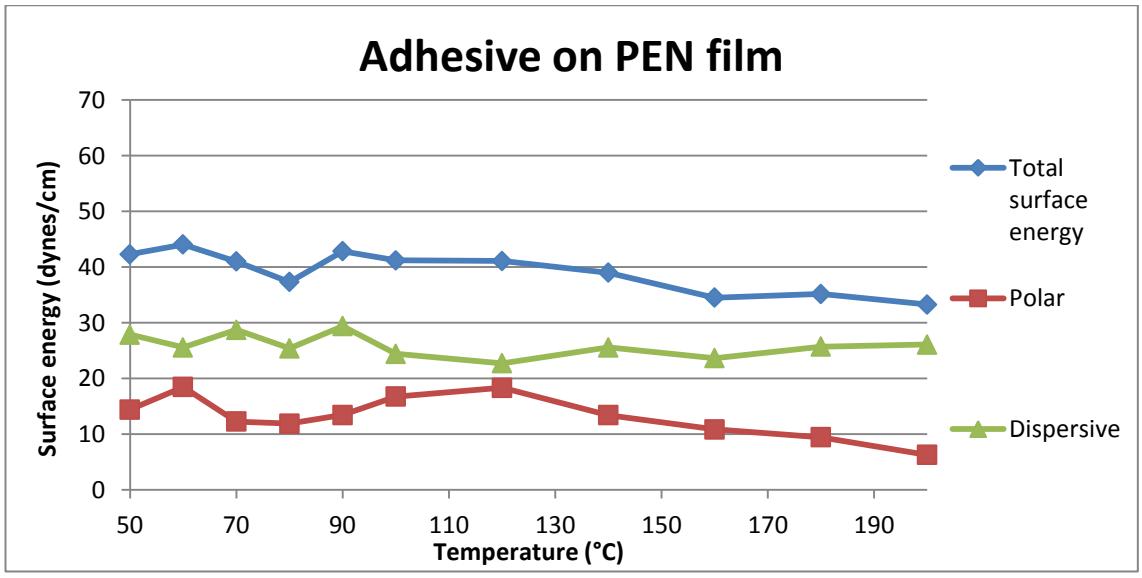

Figure 17. *Total surface energy, polar component and dispersive component of adhesive on PEN film*

The surface energy of the adhesive on PEN film does not change markedly during the oven curing. The curing time of two minutes is probably not enough to heat the adhesive to equilibrium nevertheless the true temperature achieved is likely to be within 10 °C of the set value. Unlike previous experiments, there tests exposed the adhesive to air during heating and thus some oxidation may have occurred. In the literature, the

presence of oxygen has caused decrease in reactivity and incomplete curing due to the oxygen inhibition of radical polymerization [30]; [31]. This may explain why no change is observed in the surface energy.

Work of adhesion can be calculated when the surface energy of two surfaces are known. The purpose of the work of adhesion calculations was to determine if the work required to separate the adhesive from PEN and glass changes after curing. The samples used in the calculations were the adhesive on PEN film after being laminated and cured below 80 °C and the adhesive on glass slide (AG samples). Initially the surface energy of glass and PEN film were measured before and the values of those can be seen in Table 2. The surface energy of adhesive cured at different temperatures was measured previously and the results are collected in Table 3.

Table 3. *Dispersive component, polar component and total surface energy of adhesive after curing at different temperatures*

Adhesive	Dispersive component	Polar component	Total surface energy
After curing at 50 °C	38.18	17.13	55.31
After curing at 60 °C	39.23	17.46	56.69
After curing at 70 °C	41.60	7.17	48.77
After curing at 80 °C	35.72	27.47	63.19
After curing at 90 °C	42.69	28.09	70.77
After curing at 100 °C	42.65	27.87	70.53
After curing at 120 °C	44.38	26.33	70.71
After curing at 140 °C	44.38	26.29	70.67
After curing at 160 °C	43.78	27.26	71.04
After curing at 180 °C	48.65	22.8	71.45
After curing at 200 °C	44.97	26.53	71.5

The work of adhesion was calculated for adhesive-glass and adhesive-PEN film surfaces using equation (9). The results were plotted in the graph seen in Figure 18.

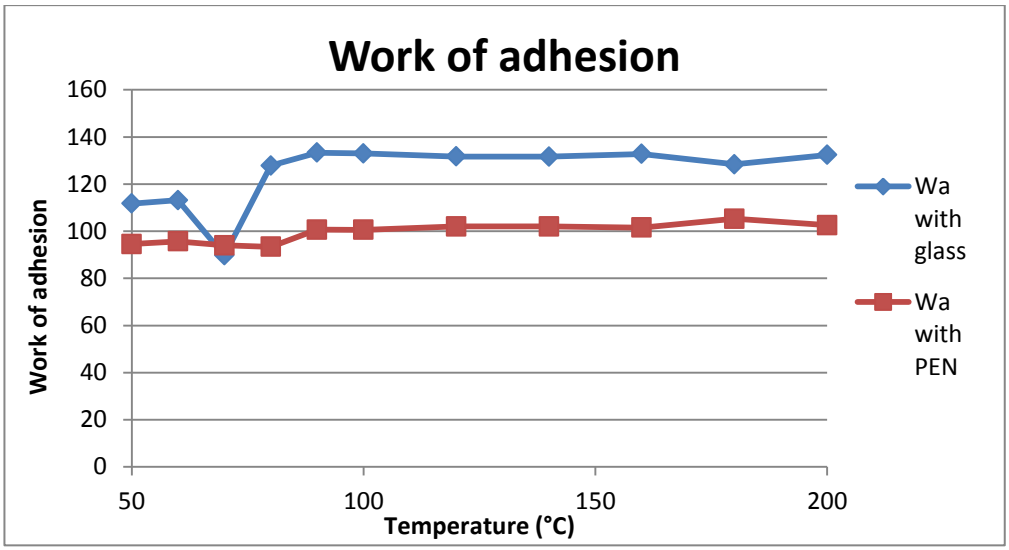

Figure 18. *The work of adhesion between adhesive-glass and adhesive-PEN film surfaces*

From the graph it can be seen that work of adhesion is fairly similar between adhesive-glass and adhesive-PEN film when the curing temperature is below 70 °C. However, the work of adhesion between adhesive and glass increases when the curing temperature is above 80 °C. The work of adhesion between adhesive and PEN film stays about the same and it is not dependant on curing temperature. This change in work of adhesion coincides with the physical phenomenon of the adhesive remaining on the glass slide after peeling.

4.2 Fourier Transform Infrared Spectroscopy

To compare the FTIR-ATR spectrum of different samples and analyse the effect of curing temperature, the spectrum of each sample was compared in the same graph and a few were selected to closer inspection. The samples AP90, AP120, AP180 and AP200 were selected because their spectra seemed to show the most variation. The FTIR spectra are shown in Figure 19.

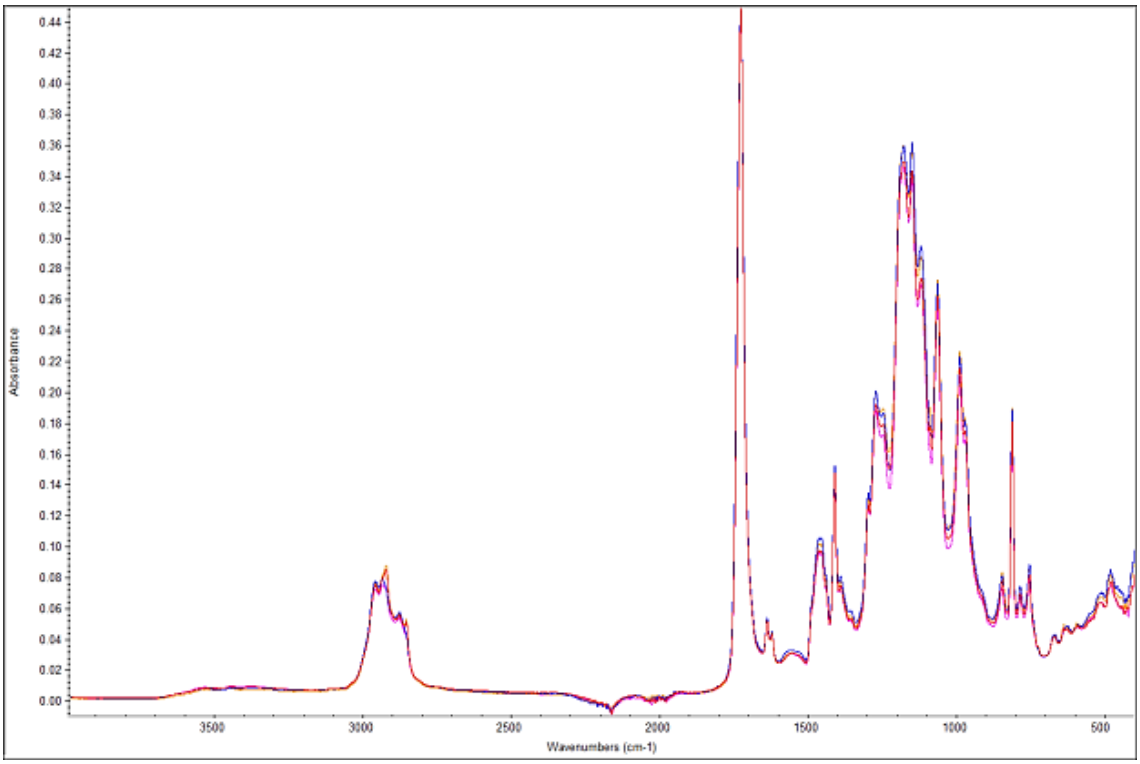

Figure 19. *The FTIR-ATR spectra of the adhesive layer on AP90, AP120, AP180 and AP200*

However, the spectra of the adhesive which was on the PEN film, showed no significant change when the curing temperature increased. To illustrate the similarity of spectra, and for comparison with later spectra, the peak at wavenumber ~1060 cm^{-1}, which is most likely a C-N stretch which is reported to occur at wavenumbers 1090-1020 cm^{-1}, was analysed for each sample [32] (p.11). The exact peak wavenumber was measured and the results are shown in the Figure 20 below.

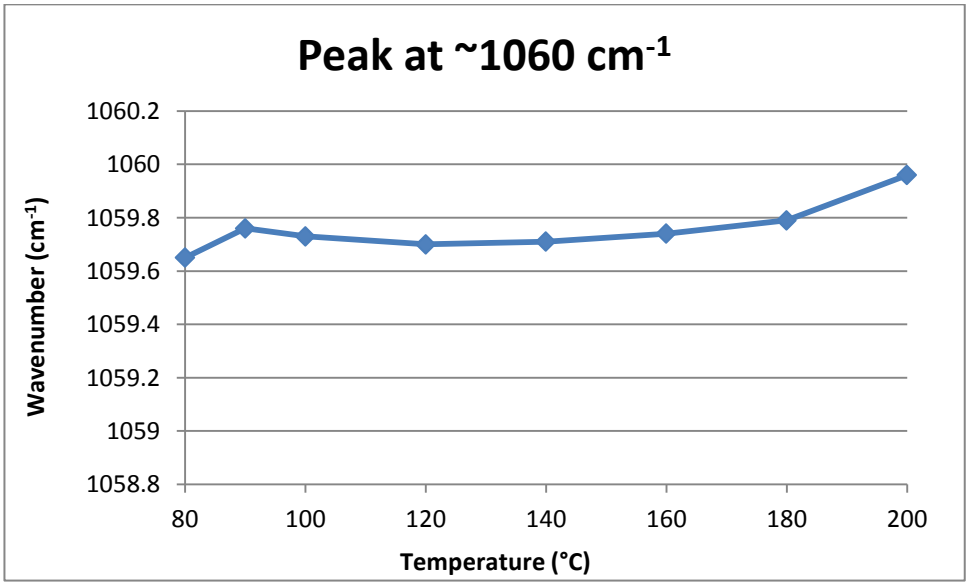

Figure 20. *The graph of the peak at wavenumber ~1060 cm^{-1}*

The peak around 1060 cm^{-1} does not show a shift to higher or lower wavelengths of more than 0.3 cm^{-1} as a result of heating between 80 °C and 200 °C. The same result is seen across the entire spectrum for different thermal histories. Thus the FTIR-ATR spectra show that no major change happens in the adhesive when it is on the PEN film and cured in the oven up to 200 °C.

The samples laminated on the glass slide and cured on a hotplate were also investigated by comparing the spectra of all samples. The full spectra of the adhesive layer on the glass slide after peeling of four different samples are shown in Figure 21.

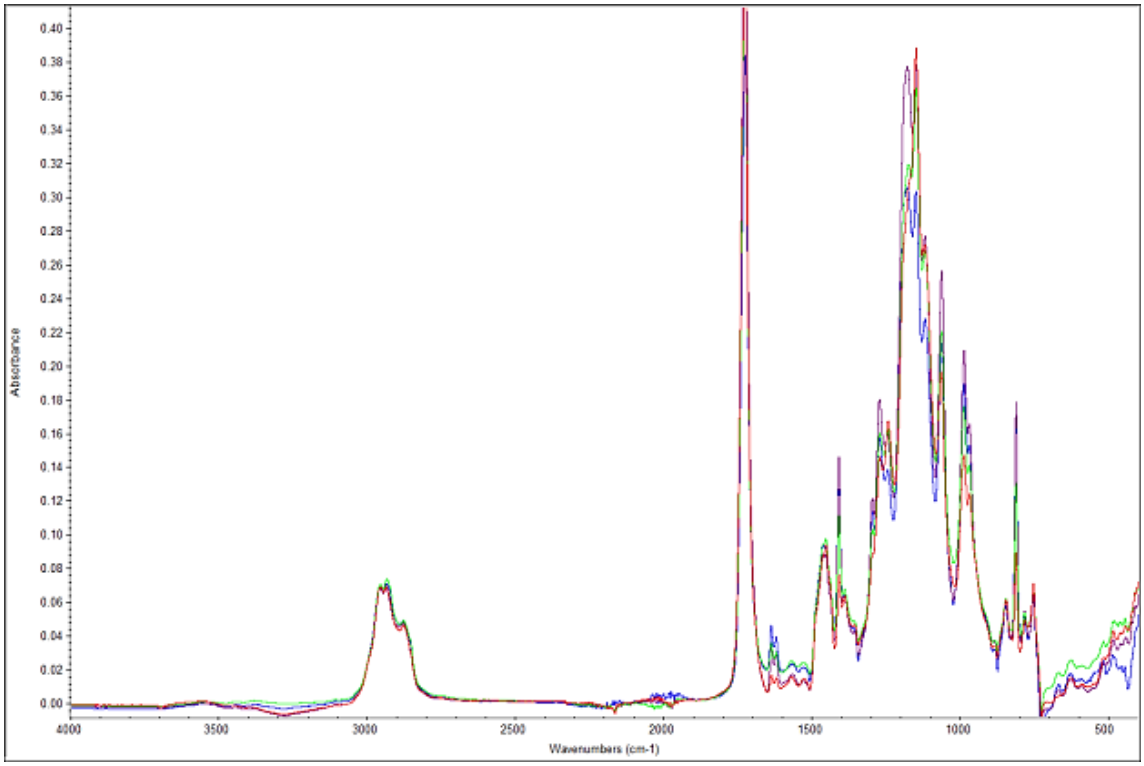

Figure 21. *Spectra of adhesive coating on glass, samples AG90 (blue), AG120 (purple), AG180 (green) and AG200 (red)*

Broadly speaking, the spectra of the adhesive in Figure 21 are similar to those shown in Figure 19. However, close examination shows that changes of peaks are happening in wavenumbers 1500–500 cm^{-1} which is in the fingerprint region. To characterise more accurately the changes, the peaks from wavenumbers 1060 cm^{-1}, 1150 cm^{-1}, 1175 cm^{-1}, 1243 cm^{-1} and 1269 cm^{-1} were compared with the sample curing temperature. Figure 22 shows an enlarged image of the peak in the region 1060 cm^{-1}.

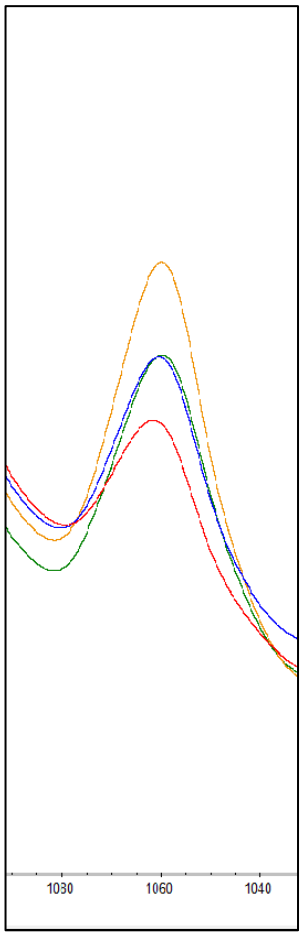

Figure 22. *Peak 1060 cm^{-1} of samples AG90 (green), AG120 (yellow), AG180 (blue) and AG200 (red)*

From Figure 22 it can be seen that the peak maximum shifts to higher wavenumbers when the sample cure temperature is increased. From each sample spectrum the exact peak position was measured and the results plotted in a graph. The graph is shown in Figure 23.

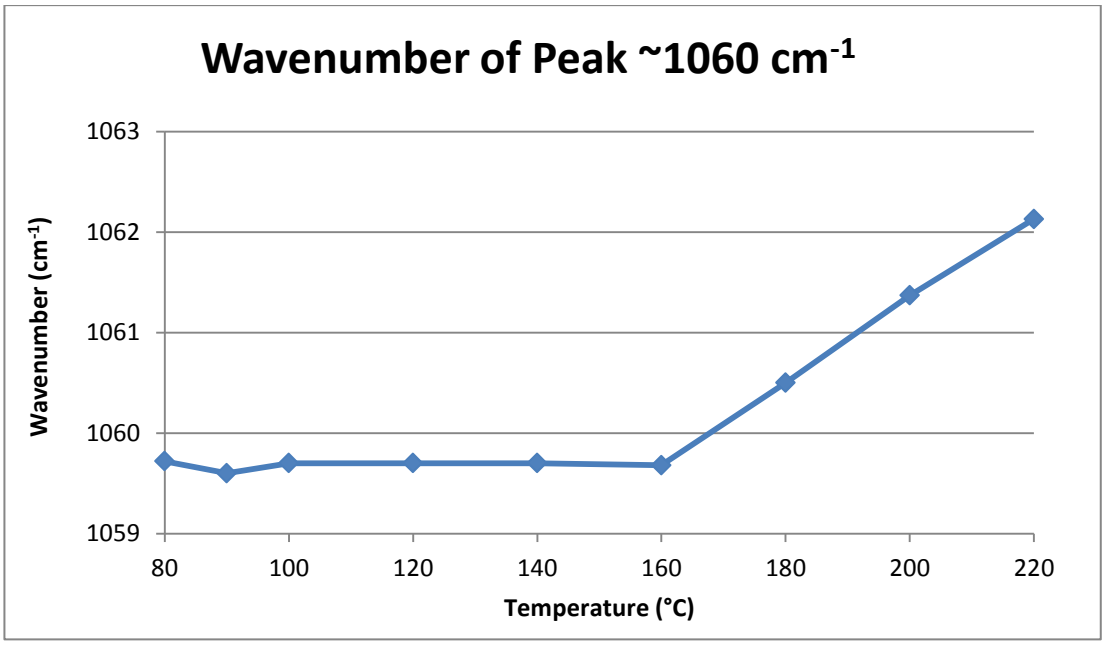

Figure 23. *Wavenumber of peak ~1060 cm^{-1} maximum*

The double peak at wavenumbers 1150 cm^{-1} and 1175 cm^{-1} was also seen to change during the curing temperature increase. Both peaks were assigned to be C-O stretch [32] (p.10) and they were analysed by calculating the ratio of the areas of peaks and comparing them to sample curing temperatures. The results which were plotted in graph are shown in Figure 24.

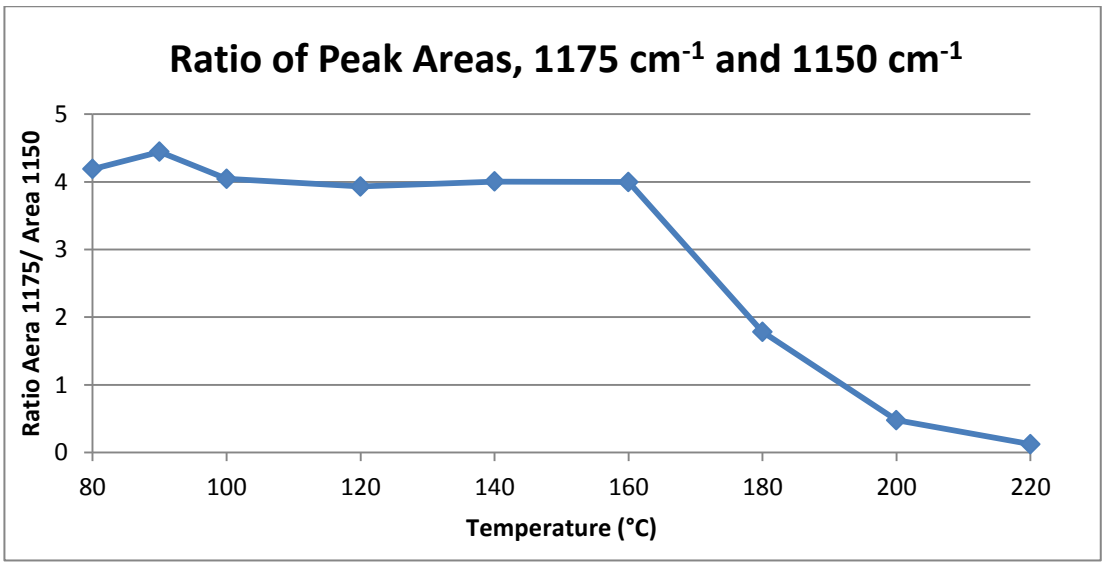

Figure 24. *Ratio of peaks 1150 cm^{-1} and 1175 cm^{-1} in different temperatures*

From the plot it can be seen that as the temperature increases the area of peak at around 1175 cm^{-1} decreases and the area of peak at 1150 cm^{-1} increases. The change in area ratios is clear so it can be concluded that there is a change in the chemical structure close to a C-O bond in the adhesive. The change in double peak can also be seen clearly from the spectra shown in Figure 25.

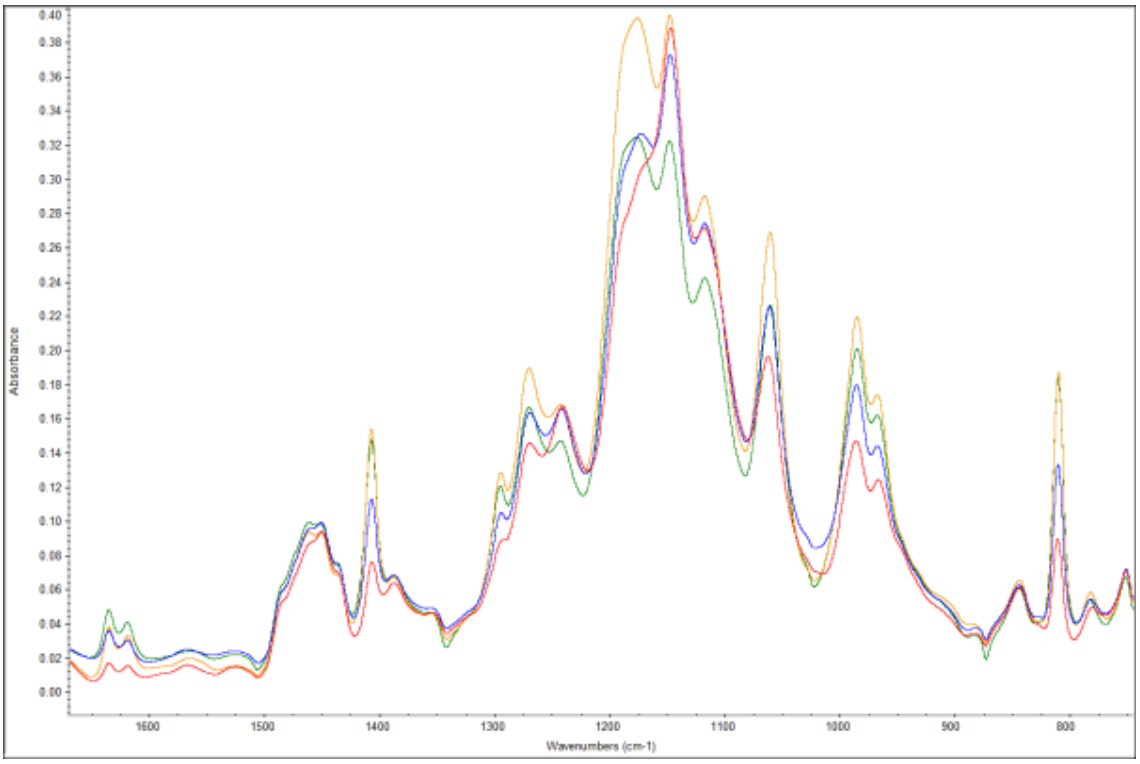

Figure 25. *Peaks 1150 cm^{-1} and 1175 cm^{-1} of samples AG90 (green), AG120 (yellow), AG180 (blue) and AG200 (red)*

The double peak at wavenumbers 1243 cm^{-1} and 1269 cm^{-1} was analysed using the same method as with the previous double peak. These peaks were also assigned as C-O stretches [32] (p.10]. The graph from the results is seen in Figure 26.

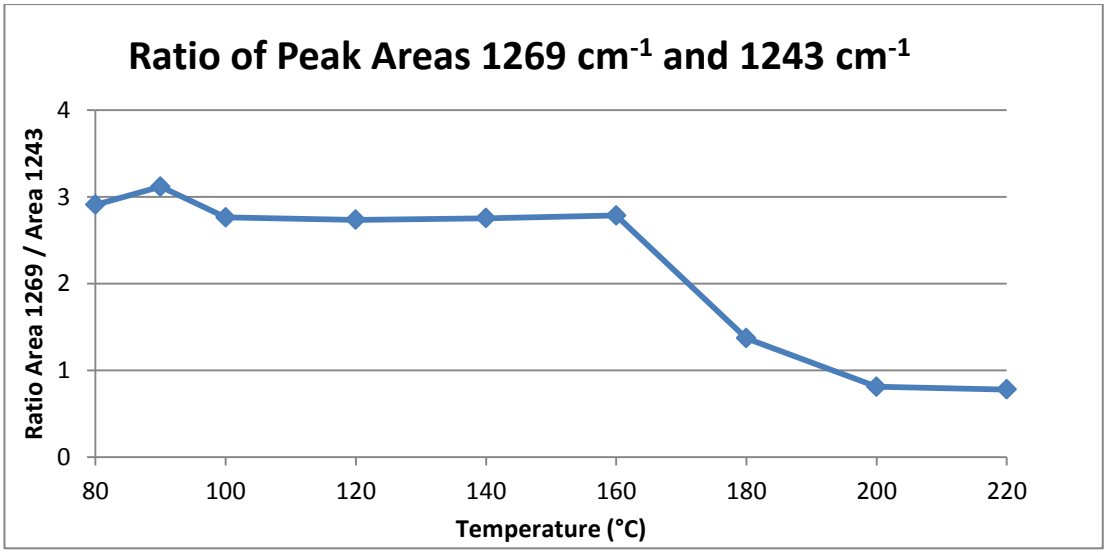

Figure 26. *Ratio of peaks 1243 cm^{-1} and 1269 cm^{-1} in different temperatures*

From the graph it can be seen that when the cure temperature is increased the area of the peak at 1269 cm^{-1}decreases and the area of peak 1243 cm^{-1} increases. This double peak change can be seen in spectra represented in Figure 25. The change of this double peak confirms that a C-O single bond within the molecular structure of the adhesive is close to or undergoes itself a chemical change, with the increasing curing temperature.

In summary, the adhesive laminated onto the glass slide and cured on a hotplate showed significant changes when the curing temperature increased. Under these conditions, the adhesive is heated but air and oxygen are almost entirely excluded. The peak at wavenumber ~1060 cm^{-1}, which is assigned to a C-N stretch, shifted to higher wavenumbers when the curing temperature approached 180 °C.

A more obvious change was observed for the double peaks at wavenumbers 1150−1175 cm^{-1} and 1243−1269 cm^{-1}. The ratio of the double peaks decreased markedly when the curing temperature increased to 200 °C. Both of the double peaks are assigned to C-O stretch and the change in the peaks may be explained by the elimination of carbon dioxide (CO_2) at high temperature. It can be speculated that CO_2 may be the product of thermal decomposition of an ester group in the adhesive, which would affect both C=O and C-O stretch bands in the infrared region. In this work heating the samples on a hotplate caused bubbling in the laminate when the temperature reached to 180 °C and this might be caused by the formation of CO_2.

In contrast, FTIR indicates that for the AP sample series, there are no major chemical changes to the adhesive on the PEN film with temperature. These samples were cured in an air circulating oven and no lamination was involved. This result entirely agrees with those of the corresponding surface energy measurements. The presence of air during curing gives the appearance that little change occurred in the adhesive.

4.3 Peel Test

4.3.1 Peel Test for Laminates

The quality of the laminates after lamination was investigated by eye and it was judged to be very good for all samples. The laminate quality after curing was assessed to be very good for all samples cured below 180 °C. During the curing on a hotplate the adhesive started to bubble when the temperature of the hotplate reached to 180 °C. At 180 °C the quality of laminate was assessed to be good and at 200 °C the quality was assessed to be okay because of high level of bubbling.

The subsequent peel of the film from the adhesive followed a stick-slip peel mechanism. The peel became smoother when the curing temperature increased. An example of the peel graph of where the peel occurred as stick-slip peel is seen in Figure 27.

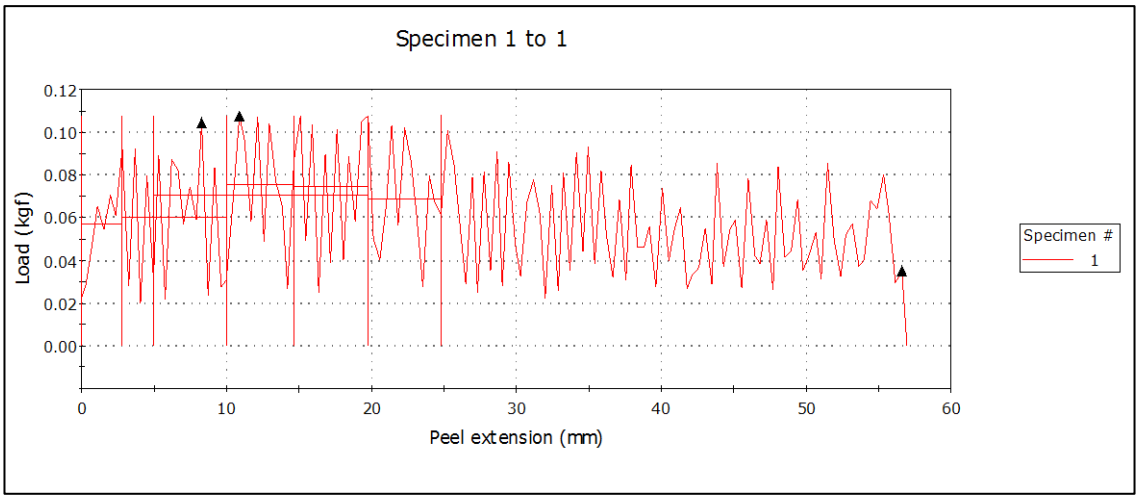

Figure 27. *Peel graph of sample cured on a hotplate at 120 °C*

From the peel graph it can be seen that the maximum and minimum value of the peel strength varies considerably. This is why maximum peel strength is not the most reliable value when comparing the peel strength between different samples. The average value of peel strength was taken from the distance between 5 mm and 20 mm where the peel was observed to be the most consistent and the standard deviation between samples is smaller than it is with maximum peel strength. Both the maximum and average peel strength from the first set of samples cured on a hotplate for two minutes at temperatures 80 °C to 200 °C are plotted in the graph seen in Figure 28.

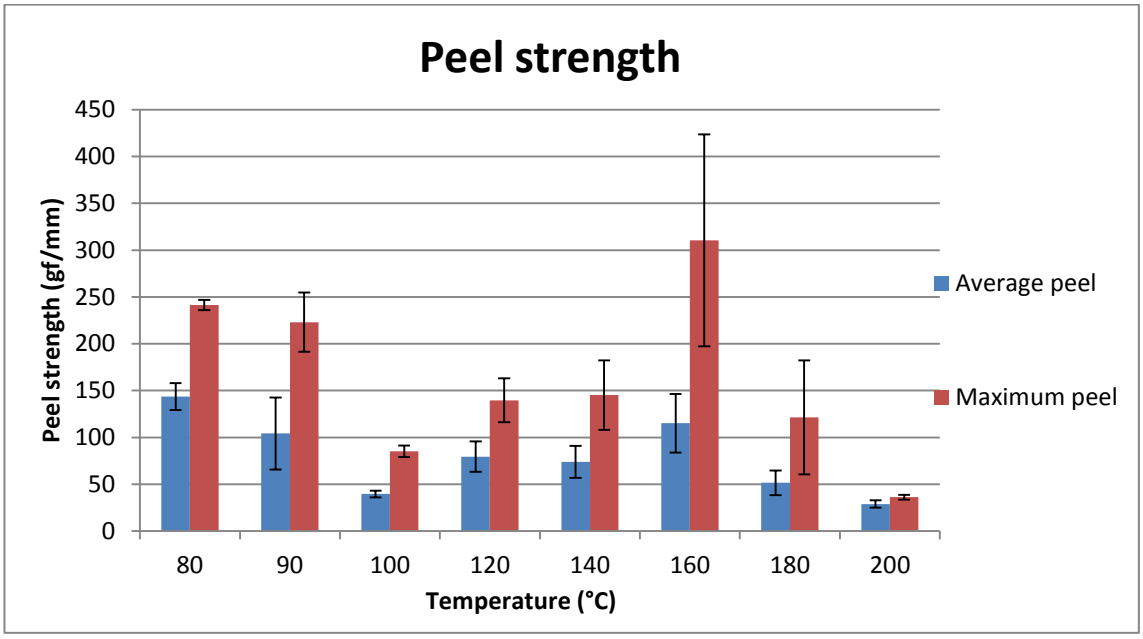

Figure 28. *The peel strength of laminates cured in the oven for 2 minutes (error bars show standard deviation)*

The percentage of bubbles in laminates cured in temperatures 180 °C and 200 °C was calculated using the image analysis program ImageJ. The area fraction of bubbles at 180 °C cured laminate was 0.043 and at 200 °C cured laminate the area fraction was 0.707. Corrected peel strength values were calculated by dividing measured peel strength by adhesive area fraction. The corrected results are shown in Figure 29.

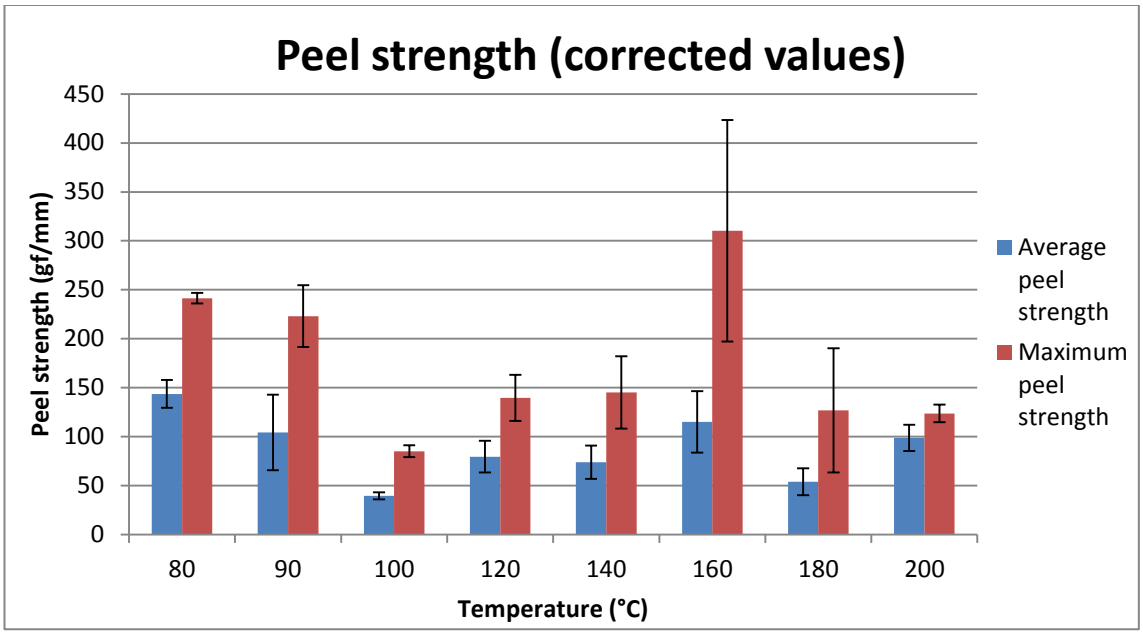

Figure 29. *The peel strength of laminates cured in the oven for 2 minutes when the bubbling is removed from the results (error bars show standard deviation)*

From the graph above it can be seen that the average peel strength first decreases until the curing temperature reaches 100 °C and after that it increases to 120 °C. However, no trend can be observed after curing temperature 120 °C. The low peel strength after curing temperatures 180 °C and 200 °C without the bubble area fraction calculations is most likely caused by the degradation of adhesive. The bubbling observed at these temperatures also indicates that a degradation reaction has occurred. After the bubbling effect has been removed, the peel strength of adhesive shows similar values with curing temperatures 120 °C and 140 °C.

The laminates were also cured in the air circulating oven and the peel strength of these samples again studied. The quality of the laminate remained very good until the curing temperature reached 180 °C. The quality of samples cured at 180 °C for two hours were assessed to have deteriorated because the film was brittle and yellow after curing. When the curing temperature was 20 min and 1 hour at 180 °C there were no visible changes at the laminates so the quality was assessed to be very good. The quality of laminate cured in 200 °C for twenty minutes was also very good and there were no visible changes in the laminates. However, when the curing time increased to one hour it caused decreasing of laminate quality and the film changed to brittle and yellow. The film could not be peeled off from the glass slide because of the brittleness and therefore

peel value could not be measured from these samples. From all the other samples the average peel strength was plotted in the graph seen in Figure 30.

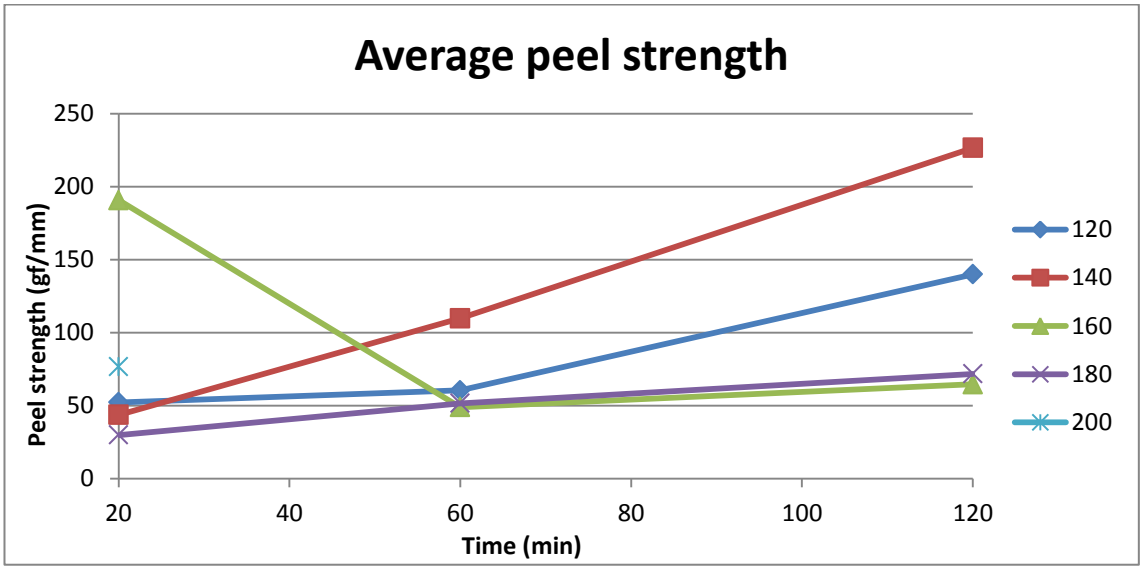

***Figure 30**. Average peel strength of oven cured samples*

From the graph it was seen that the peel strength increases with time at temperatures 120 °C and 140 °C. However, at temperature 160 °C the peel strength is seen to decrease from curing time 20 min to 1 hour. The samples cured at 180 °C did not show any major change over the time. From this graph no significant conclusions of the behaviour of adhesive in different temperatures could be made.

To study the time-temperature behaviour more accurately, the curing times and temperatures were changed. The new set of samples was cured in oven from 10 min to 60 min at 10 min increments. The laminate quality was very good for all the samples and no bubbling occurred even at 180 °C. The average peel strength of these samples was plotted to graph seen in Figure 31.

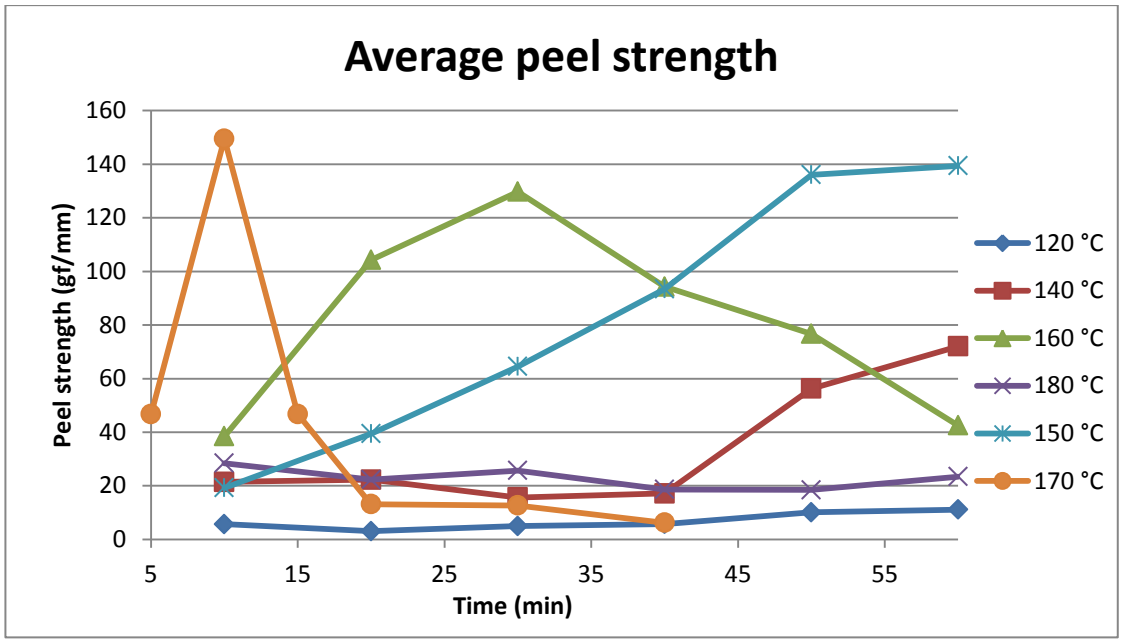

Figure 31. *Average peel strength of oven cured samples*

From the time-temperature curve it can be seen that peel strength starts to increase when the sample is cured in oven at 140 °C for over 40 minutes. For temperatures higher than 140 °C the peel strength starts to increase after less time. However, a maximum point of peel strength can be seen at temperature 160 °C in 30 min and after that peel strength decreases again. The increase of peel strength after curing the sample at temperature 140 °C and above is most likely caused by the chemical reaction in the adhesive. The decrease of peel strength that is seen after prolonged curing at 160 °C and 170 °C may be due to degradation of the adhesive which follows the initial change.

4.3.2 Peel Test for Adhesive Cured at Low Temperatures

To measure the peel strength between the PEN film and the adhesive at low curing temperature, the laminate and peel test had to be redesigned. Epoxy glue was used to stick the adhesive to another PEN film before peeling. The measurements were performed at a peel angle 180° instead of 90° like before. The average peel strength was calculated from a sample between peel distances of 10 mm and 40 mm. The peel strength at different curing temperatures was plotted in the graph seen in Figure 32.

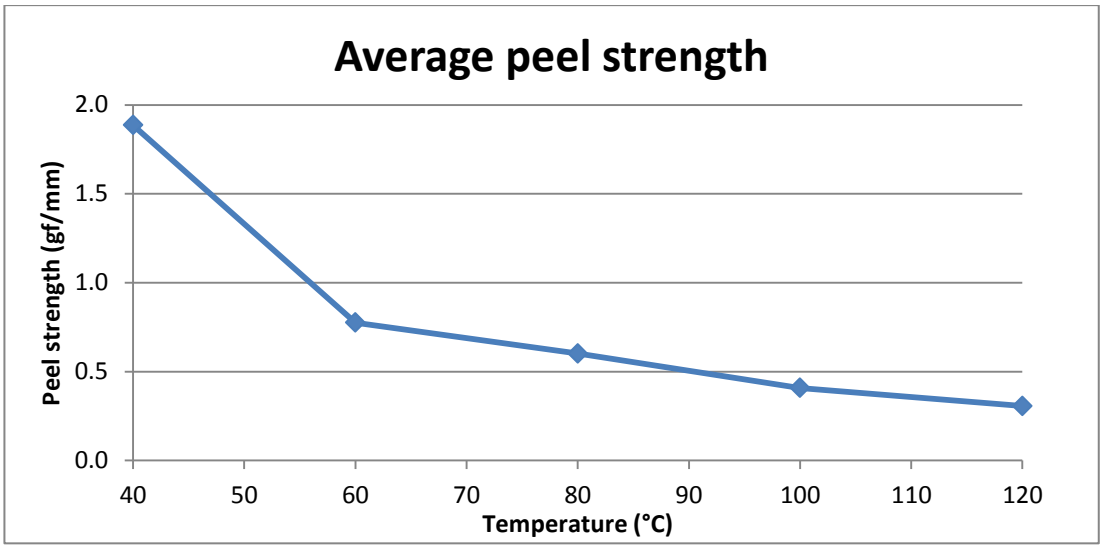

Figure 32. *Average peel strength in different curing temperatures*

From the graph it can be seen that the peel strength decreases when the temperature increases. From this it can be concluded that the adhesion between the PEN film and the adhesive decreases when the curing temperature increases. This helps the switching effect that occurs when curing temperature reaches 80 °C. The peel strength measured is markedly lower than the peel strength of laminates. However, these peel strengths cannot be directly compared as the peel angle affects the measured peel strength such that when peel angle is increased the peel strength decreases [33].

The interfaces generated from these peel experiments were investigated using surface energy measurements to ensure that the measured peel strength is between the PEN film and the adhesive. By examine the surfaces by eye the PEN film seemed to be clean from adhesive and epoxy. However, it was difficult to see if the adhesive was on the other peeled surface. The surface energy values of the peeled interfaces were plotted and they can be seen in Figure 33.

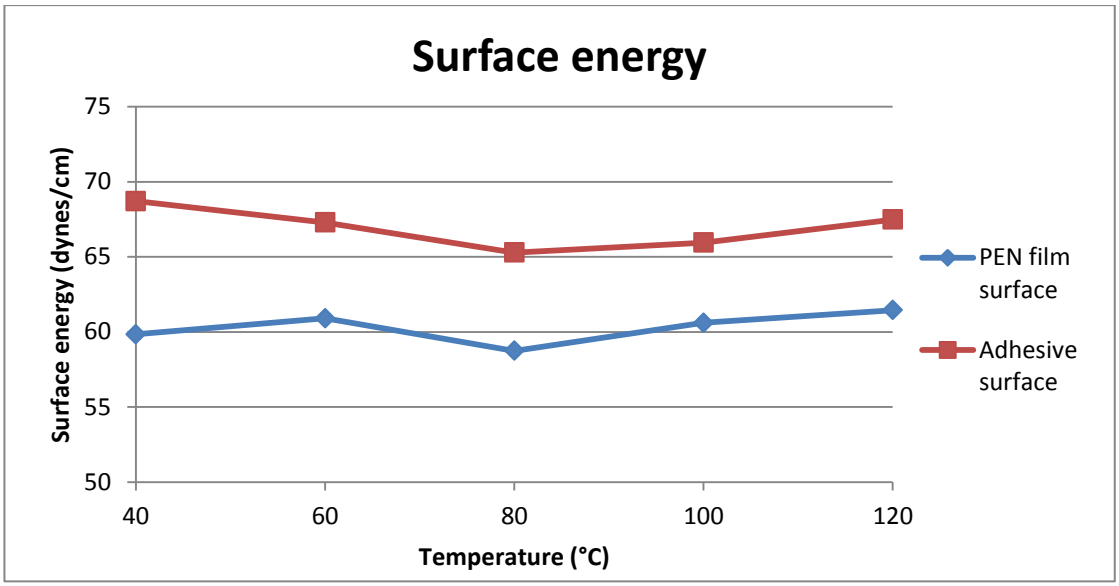

Figure 33. *Surface energies of peeled samples on both interfaces*

The surface energy of the PEN film exposed after peeling is slightly higher than the surface energy measured for pure PEN film. This may indicate that there are some residues from the adhesive on the surface of the peeled PEN film. The surface energy of the adhesive exposed after peeling is about the same as that measured before from the adhesive on the glass slide. However, the adhesive cured below 80 °C showed markedly lower value of surface energy (~50 dynes/cm) in the previous measurements on the PEN film and it can be argued that the surface exposed in these measurements is not a pure adhesive. The exposed adhesive surface was also measured using FTIR-ATR to see if the epoxy glue had affected the adhesive surface. The FTIR spectra from the samples cured in 40 °C, 100 °C and 120 °C are seen in Figure 34.

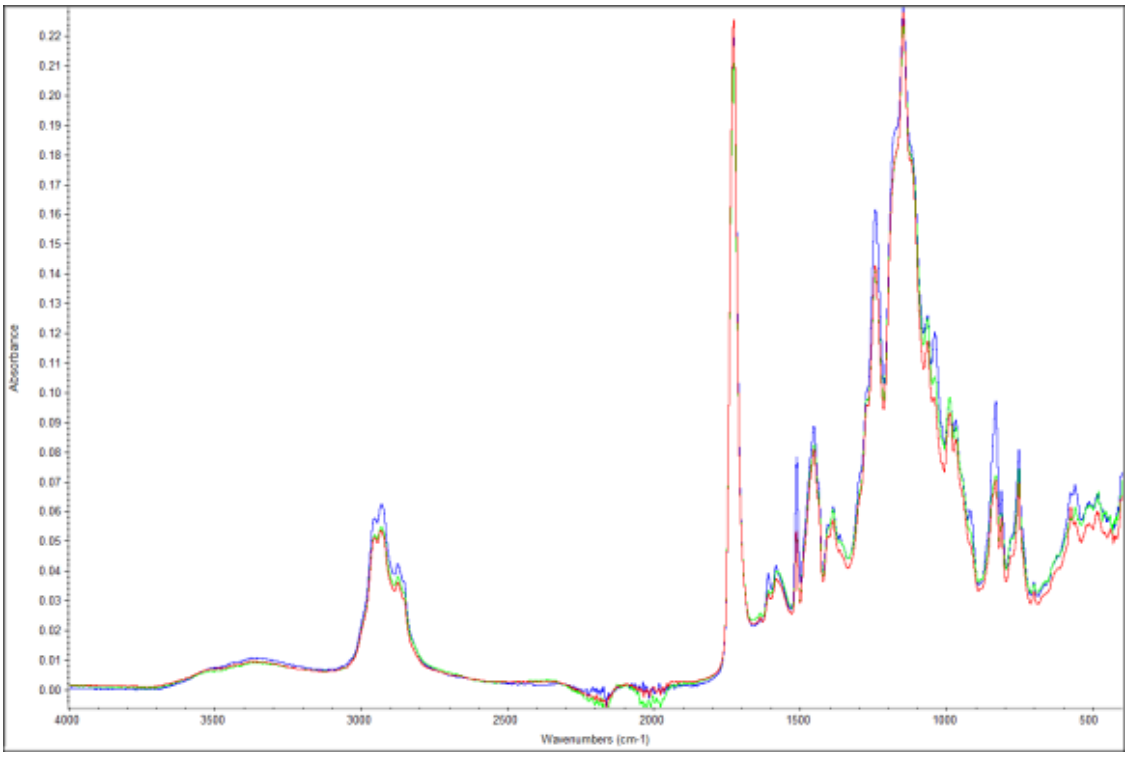

Figure 34. *FTIR spectra of adhesive interface (blue 40 °C, red 100 °C, green 120 °C)*

The spectra from the samples cured at different temperatures are broadly speaking the same. However, the spectra differ from the FTIR spectra measured before on the PEN film and on the glass slide. Therefore, it is possible that the adhesive interface comprises some migrated epoxy glue and the measured peel strength is affected by the epoxy glue. This would tend to emphasize the low peel strength values measured with 180° peel test.

4.4 Thermal Analysis

4.4.1 Differential Scanning Calorimetry

From the first samples measured with DSC (heating program described in Chapter 3.5.1) the second heating scans were analysed. The second heat scans, which were put through the same end temperature in the first heat scan, were compared in the same graph. The scans from the second heating, after heating the samples at 120 °C for 10 min, 30 min and 60 min, are presented in Figure 35.

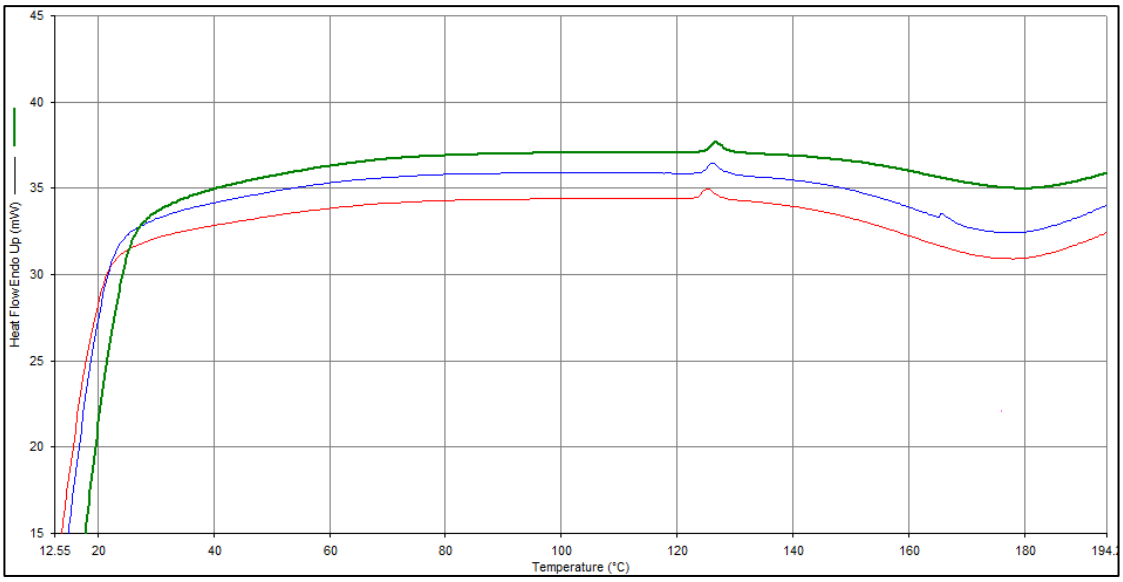

Figure 35. *120 °C cured adhesive, red: 10 min, blue: 30 min, green: 60 min*

The curves in Figure 35 look rather similar and a peak at circa 125 °C can be seen in all of the curves. The adhesive prepared is semicrystalline and at 125 °C the crystallisation is most likely starting to melt resulting in a melt peak. When the cooling rate of 50 °C/min is used, the crystallisation is occurring during cooling and with the second heating the melt peak is detected again. After the melt peak, around 140 °C, the scans show a drop in heat flow. This drop is possibly due to the degradation and crosslinking of the adhesive. The area of possible degradation is analysed from scans heated first to 120 °C, 130 °C and 140 °C. Areas were plotted to graph with heating time seen in Figure 36.

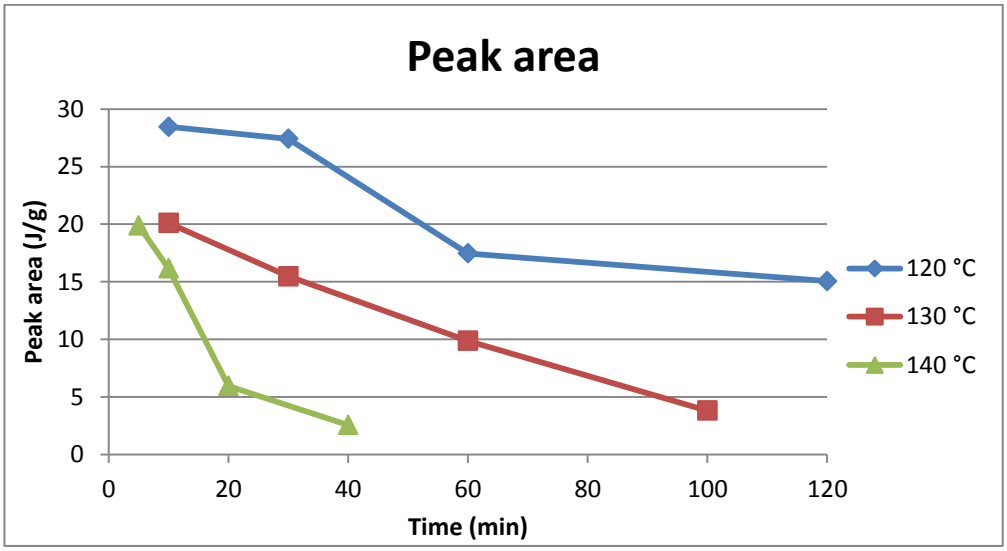

Figure 36. *Degradation area of the second heating scans*

The degradation area is seen to decrease with the increasing heating time and higher temperatures. This reaction is most likely the same as that detected with FTIR and peel

test. With DSC the reaction seems to occur from temperature 120 °C, which is presumably caused by the adhesive being heated in its casted form instead of being laminating on the glass slide with PEN film. The second heat scans of the samples heated first to 150 °C for 10 min, 30 min, 1 hour and 2 hours, are seen in Figure 37.

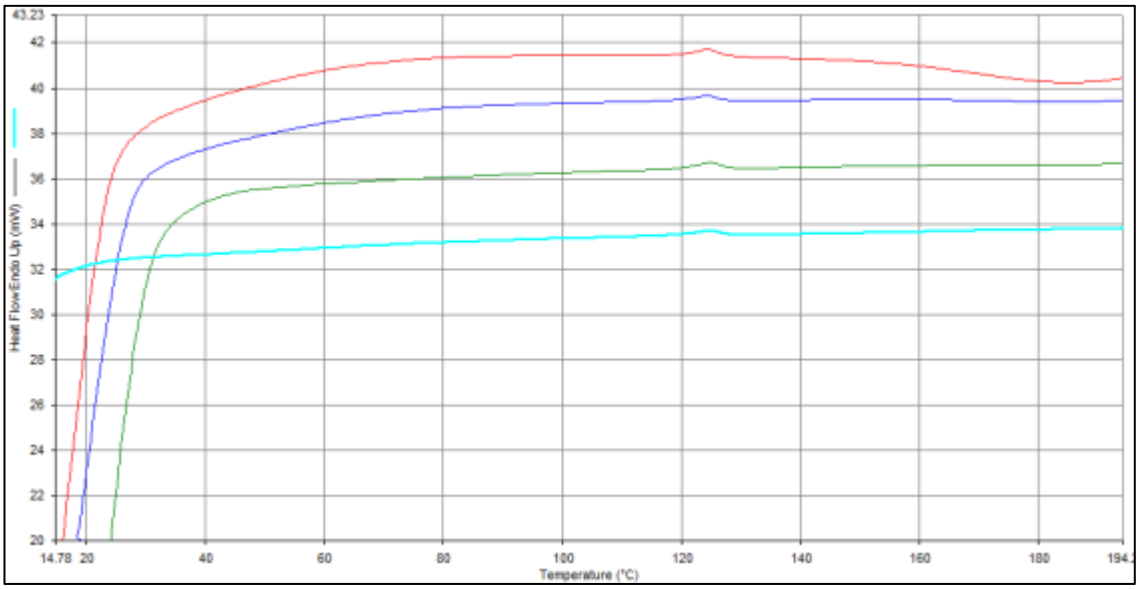

Figure 37. *150 °C cured adhesive, red: 10 min, blue: 30 min, green: 60 min and light blue 120 min*

From the Figure 37 it is seen that the degradation reaction at 140 °C is only detected for the sample kept at 150 °C for 10 minutes. This indicates that the reaction after 140 °C is an irreversible reaction and after 10 minutes of heating at 150 °C the adhesive has not completely gone through the reaction. Additionally, the melt peak at around 125 °C is seen to decrease when the sample has been held in the end temperature of first heating scan for longer time. The second heating scans of the samples heated first to 170 °C were also analysed. The scans are seen in Figure 38.

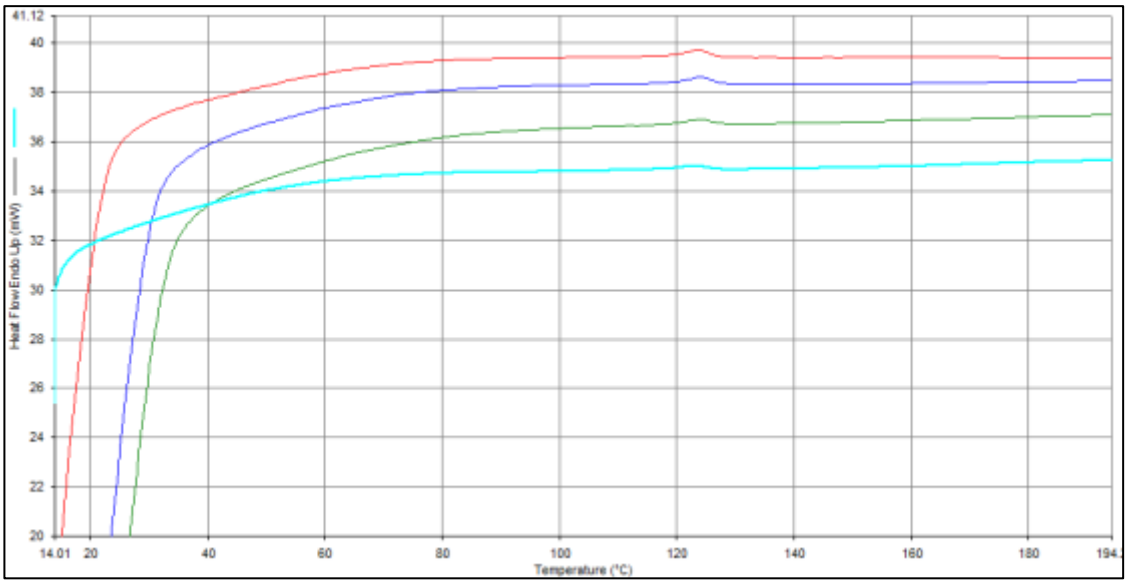

Figure 38. *170 °C cured adhesive, red: 10 min, blue: 30 min, green: 60 min and light blue 120 min*

The scans in Figure 38 seem fairly similar with the scans seen in Figure 37. Again, no degradation has occurred in the samples heated first to 170 °C. The melt peak is seen around 125 °C and the area of peak is decreasing as with samples heated first to 150 °C. The area of peak at circa 125 °C was calculated from the scans at both temperatures where the melt peak area was seen to change. The results were plotted to graph with holding time seen in Figure 39.

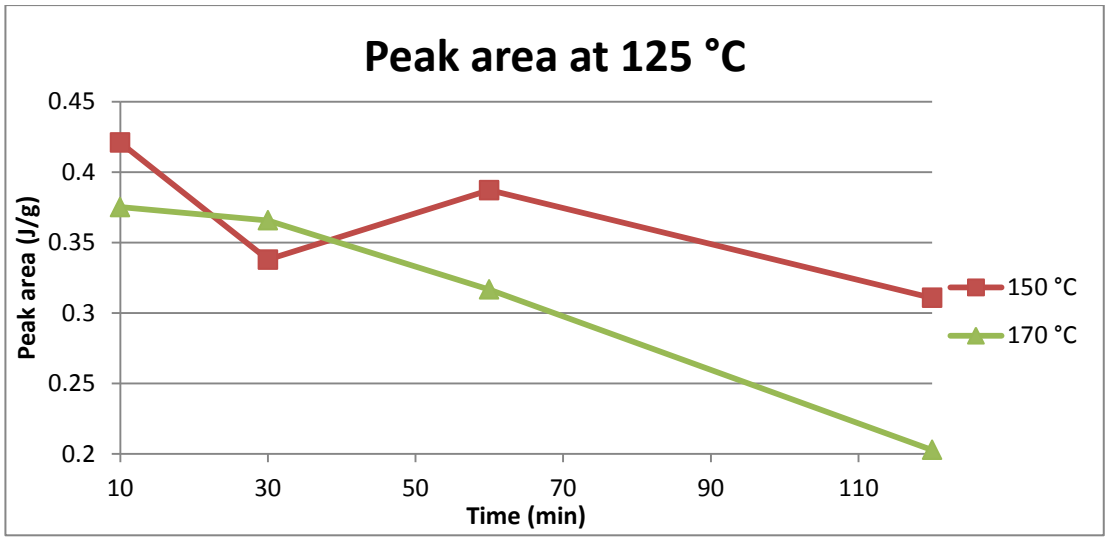

Figure 39. *The peak area at 124 °C for the adhesive first heated to temperatures 150 °C and 170 °C for different times*

From the graph above it can be seen that the peak area decreases when the curing time increases. Also the peak areas of samples heated to 150 °C is seen to be higher than of the samples heated to 170 °C. The peak area change is most likely caused by the irreversible reaction occurring after 140 °C. Because of the irreversible reaction, the

crystallisation of the adhesive decreases during the cooling and that is why the melt peak also decreases when the heating temperature and time increases. It would appear that by curing for longer times and at higher temperature a chemical change occurs which alters the chemical structure of the adhesive sufficiently to retard or prevent crystallisation of regular structural features in its molecule.

The glass transition temperature was not seen in the graphs measured before so it was assumed that the adhesive undergoes glass transition at lower temperatures. For measuring the glass transition temperature the adhesive was tested using a different heating program which started from -80 °C. The graph from glass transition measurement is seen in Figure 40.

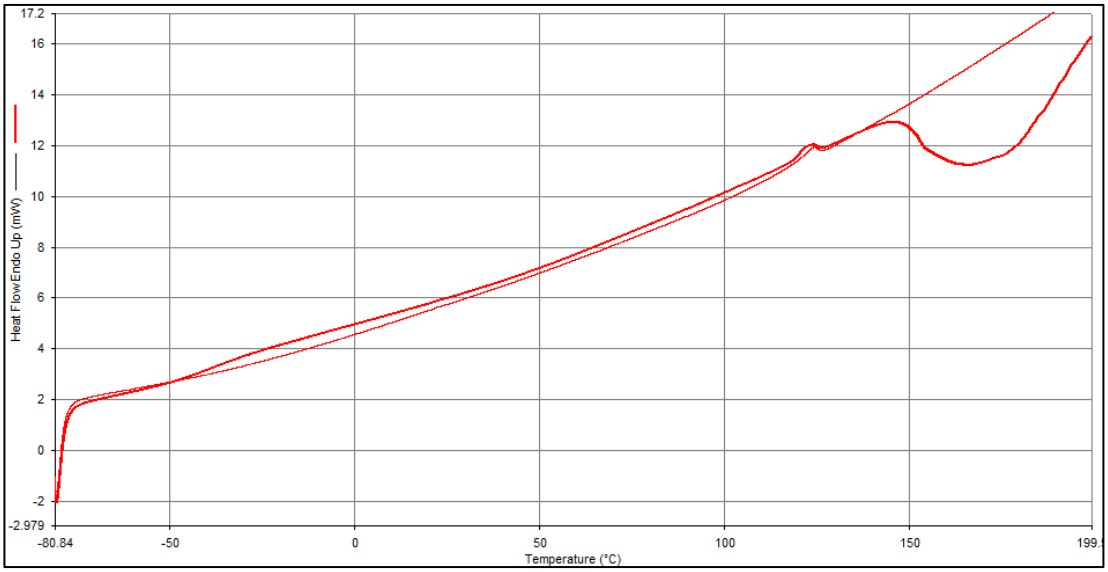

Figure 40. *First heating scan (highlighted) and second heating scan of adhesive*

From the first heating scan, which is the highlighted graph, the glass transition temperature can be seen between the temperatures -50 °C and -40 °C. The second heating scan does not show a clear glass transition step so the first heating affects the properties of the adhesive. The melt peak observed at temperature circa 125 °C occurs in the both heating scans but the cooling curve does not show a crystallisation as the samples are ballistic cooled. The crystallisation is most likely taking place in the second heating. However, the crystallisation occurs over a very broad temperature range and the amount of crystallisation is so small, that it cannot be seen in the second heating scan. After temperature 140 °C the graph is observed to have a major drop, which is the irreversible reaction caused by a chemical change or degradation which might involve crosslinking.

The change in T_g in the second heating was assumed to be due to the degradation reaction occurring after 140 °C. To demonstrate that the change does not happen after initial heating to a lower temperature, the adhesive was first heated to 120 °C instead of the previous 200 °C. The scans from the measurements are seen in Figure 41.

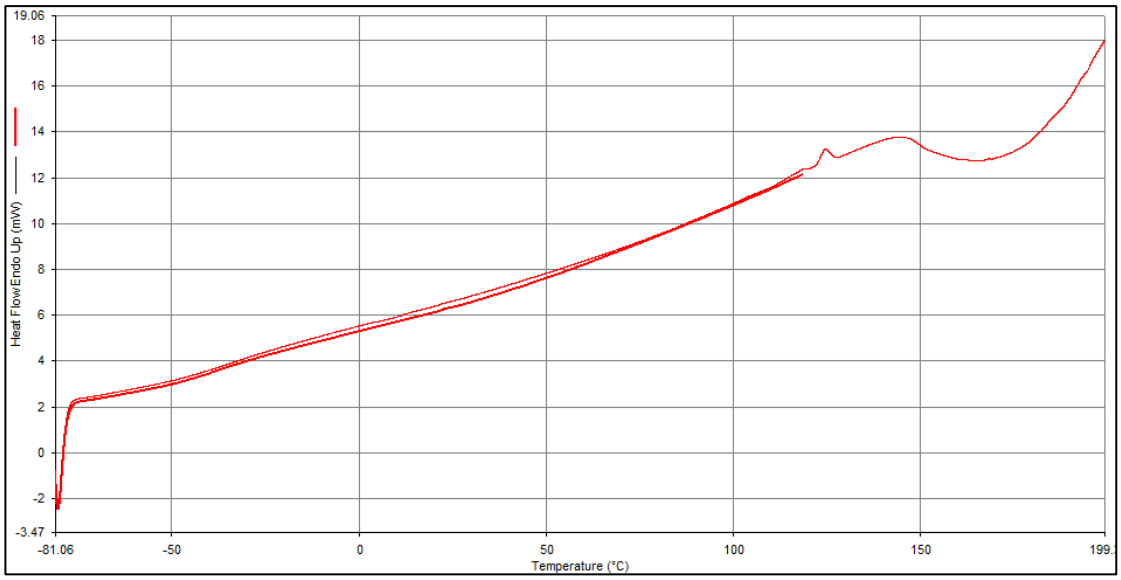

Figure 41. *First heating scan (highlighted) to 120 °C and second heating scan to 200 °C*

From the Figure 41 it can be seen that the T_g step is observed in both cases and it does not change in the second heating. Therefore two comments can be made. The characteristic shape and reversible nature of the feature at circa -45 °C allows its assignment to be the T_g and the change in T_g at previous measurements is caused by the first heating above 140 °C, where the crosslinking and degradation reaction starts.

4.4.2 Thermomechanical Analysis

A specimen of solvent cast adhesive was first cooled to -150 °C to ensure that the sample is below its glass transition temperature, before conducting the thermomechanical analysis. The sample was the heated to 160 °C at a rate of 5 °C/min and the position of the probe was monitored continuously during the programme. The graph recorded is seen in Figure 42.

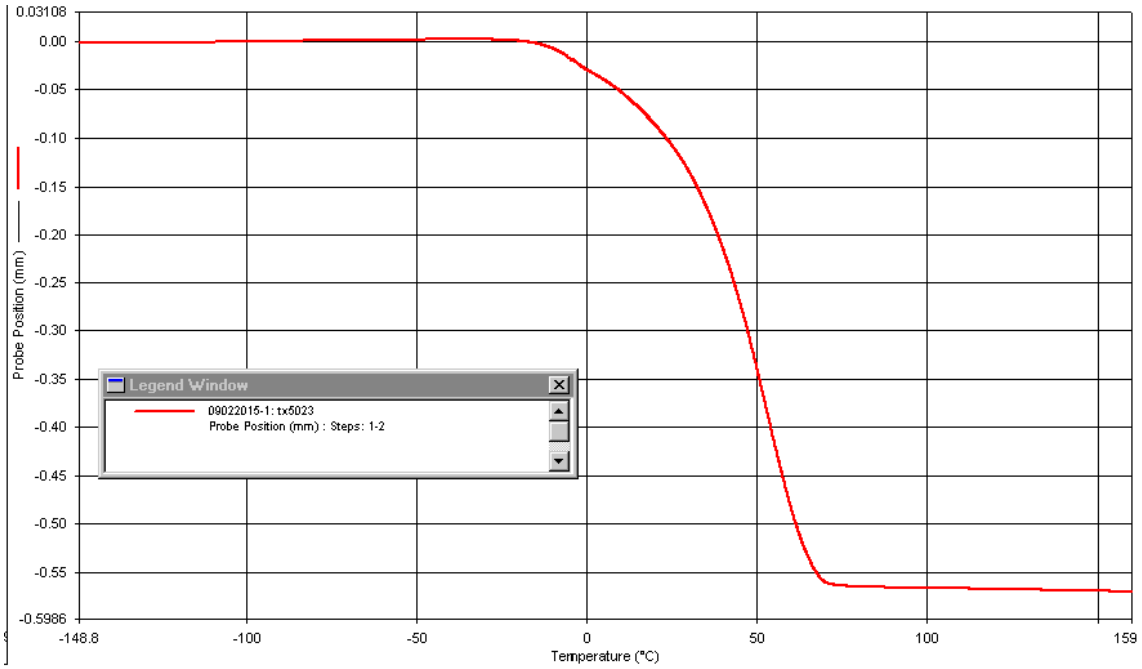

Figure 42. *Adhesive heated first time to 160 °C*

From the graph it can be seen that the probe first moves vertically upwards which is attributed to the expansion of the sample during heating. The glass transition temperature can be detected for amorphous and semicrystalline material when the material exhibits an increase in its coefficient of thermal expansion [34]. However, the tests were run with the penetration probe as the sample was too thin and soft to measure with the expansion probe. The expansion data cannot be used to indicate reliably the T_g of the sample as the probe exerts a force on the sample during its expansion. After the temperature reaches circa -20 °C the probe is seen to fall as the sample started to soften. Therefore the glass transition temperature is below the softening point and this is consistent with the DSC results. The maximum penetration of the probe into the softening sample was seen at about 70 °C. After the first heating the sample was cooled again to -150 °C and after repositioning the probe on a fresh area of the specimen a second heating was performed. The graph from second heating is seen in Figure 43.

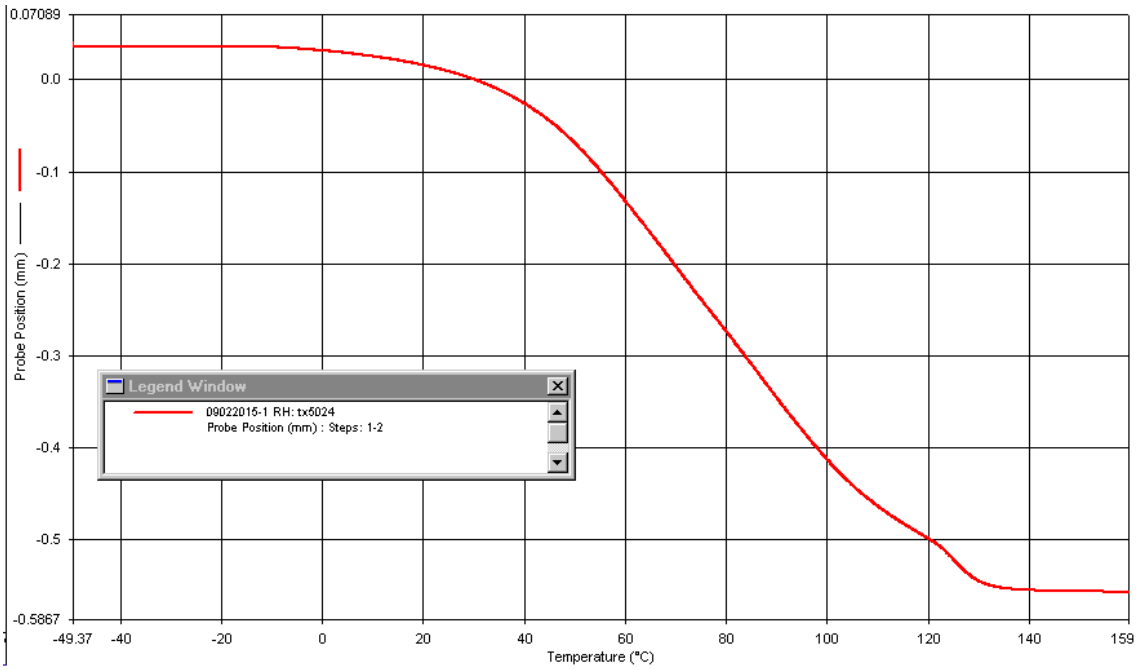

Figure 43. *Adhesive heated second time to 160 °C*

During the second heating the onset of softening appears at approximately the same temperature. However, the time and temperature required to achieve a similar depth of penetration by the probe was increased. These changes are most likely caused by the first heating to 160 °C which is the temperature range where the adhesive is seen to switch its physical behaviour in previous tests.

5. KINETICS

The chemical reaction kinetics was used to study the rate of the change in the adhesive. The goal was to derivate an equation to calculate the amount of change occurred in the adhesive after it is cured at varied temperatures and times. Instead of concentration of the material, the peak area change from FTIR spectra was used as a value of change [35], which can be related to the concentration via Beer Lamberts law as discussed later in this section.

The adhesive on PEN film was laminated on the glass slides and cured in an air circulating oven at temperatures 150 °C, 160 °C and 170 °C. The laminates were kept in an oven for various times between 5 min to 2 hours. After laminates were cooled to room temperatures, they were peeled and the exposed adhesive on the glass slide was measured with FTIR-ATR. The FTIR spectra were analysed by calculating the area of peak at 1175 cm^{-1}, which is assigned as C-O stretch. The area of peak was calculated using the same baseline with all the samples. The peak at wavenumber 1635 cm^{-1}, which is assigned as C-N stretch, was used as an internal standard as it was seen to be stable at all temperatures. The areas with curing time were plotted to graph seen in Figure 44.

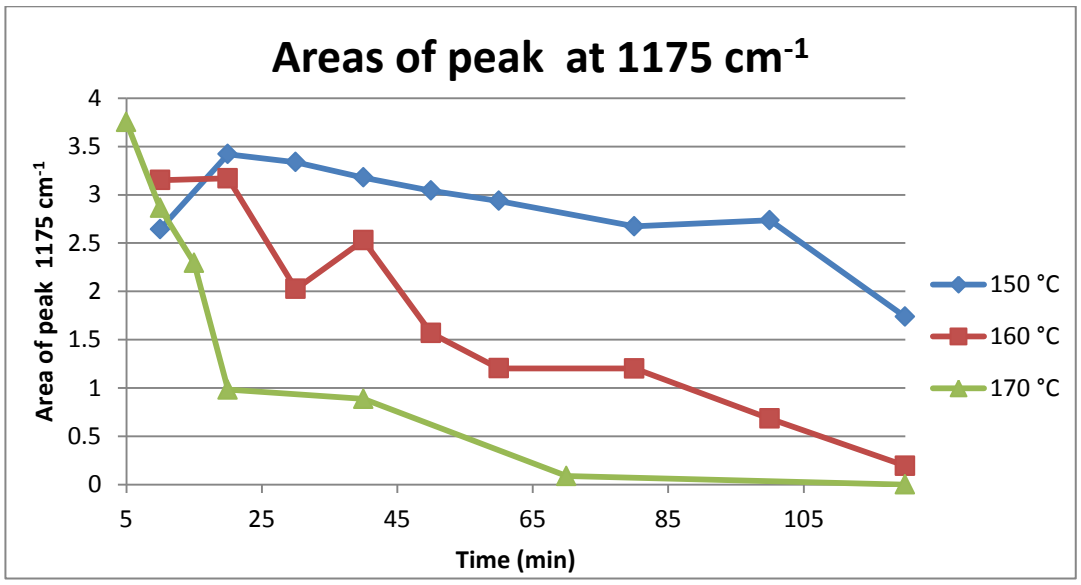

Figure 44. *The areas of peak at 1175 cm^{-1} after samples are cured in different times and temperatures*

To calculate the rate constant of the reaction, the rate of reaction r_A has to be defined first. The amount of a component A being produced per unit quantity of a reference variable y is defined as the rate of reaction. The equation of r_A can be expressed as

$$r_A = \frac{1}{y}\frac{dN_A}{dt} \quad \text{(eq. 11)}$$

where N_A is the Avogadro constant expressed as molar units and t is the time. When the volume of the reacting fluid system remains constant, the equation (11) can be written

$$r_A = \frac{d[A]}{dt} \quad \text{(eq. 12)}$$

where [A] is the concentration of component A. [36] (p.4–5)

The order of reaction is the sum of the exponents determined empirically but it may also refer to the individual reacting components. From the Figure 44 it can be seen that the change in the adhesive follows the first order reaction and the kinetic calculations can be made using the first order reaction equations. In the case of the first order reaction, where A is the reactant, the rate of reaction is

$$r_A = -k[A] \quad \text{(eq. 13)}$$

where k is the rate constant of the reaction. This assumption is confirmed by the presence of a linear relationship given by Equation 16 as illustrated later in Figures 47–49. If the reaction order with respect to reactant A was different, a non-linear relationship would be evident in these plots.

Combining the equations (12) and (13) the equation can be written

$$\frac{d[A]}{dt} = -k[A] \quad \text{(eq. 14)}$$

Using integration, the equation (14) can be expressed as

$$\int_{A_0}^{A} \frac{d[A]}{[A]} = -k \int_0^t dt. \quad \text{(eq. 15)}$$

After equation (15) is integrated, the concentration of A can be expressed as

$$\ln[A] = \ln[A_0] - kt. \quad \text{(eq. 16)}$$

where $[A_0]$ is the concentration of A after time 0. [36] (p.4–5)

In this study the concentration of the adhesive is unknown but the peak area change between samples can be calculated from the FTIR spectra so the amount of absorbance is known. The Beer-Lambert law connects the absorbance Abs and concentration c as follows

$$Abs=\varepsilon cl \quad \text{(eq. 17)}$$

where ε is the Beer-Lambert absorption coefficient, and l is the thickness of material in this study [37]. It is assumed that the Beer-Lambert absorption coefficient and the thickness are constant for the samples and therefore the absorbance equals to concentration.

The calculation of the rate constant is fairly straightforward as the rate constant can be determined by taking an average of values calculated at individual experimental points. [36] (p.15) As seen in equation (16) the rate constant is the slope of the linear plot of natural logarithm of concentration of A. In this study the natural logarithm of area was calculated and it was plotted as a function of curing time to calculate the rate constant. The graph of peak areas from samples cured at temperature 150 °C is shown in Figure 45.

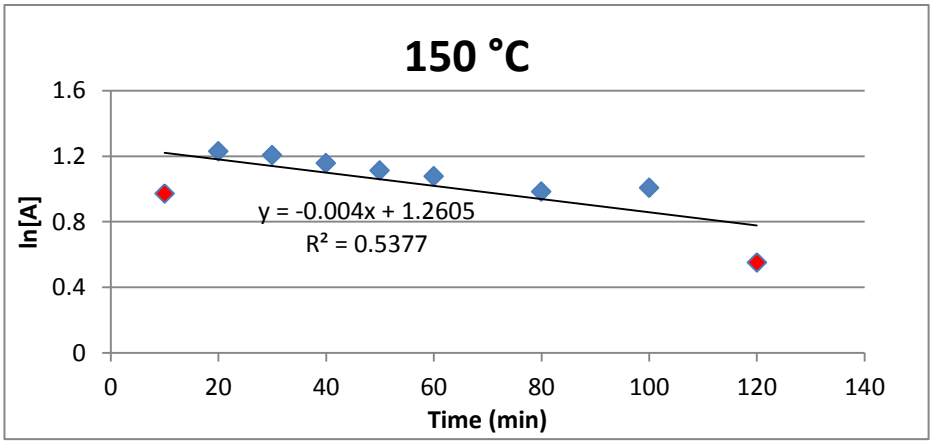

Figure 45. *The graph of samples cured in 150 °C to determine the value for rate constant*

The square of the correlation coefficient of the linear plot seen above is only 0.5377. From the graph it can be seen that the first point at time 10 min and the last point at time 120 min do not fit in the trend line with the rest of the points and they are coloured in red. The probability of these points being outliers was calculated with the statistical program Minitab. With Minitab the Standardized residual (St Resid), which is the ratio of residual standard deviation and the residual, was calculated. Minitab considers the points that have St Resid values greater than 2 as outliers. The results of the Minitab calculations are seen in Table 4.

Table 4. *The standardized residuals from the Minitab*

Obs	Time	Area	Residual	St Resid
1	10	0.9723	-0.248	-2.02R
9	120	0.5519	-0.2265	-2.12R

From the Table 4 it can be seen that the points at time 10 min and 120 min have a St Resid value of over two and that is why they can be removed from the graph. To illustrate that the removed points are outliers, the value of residual of each point was plotted to graph with Minitab. The graph is seen in Figure 46.

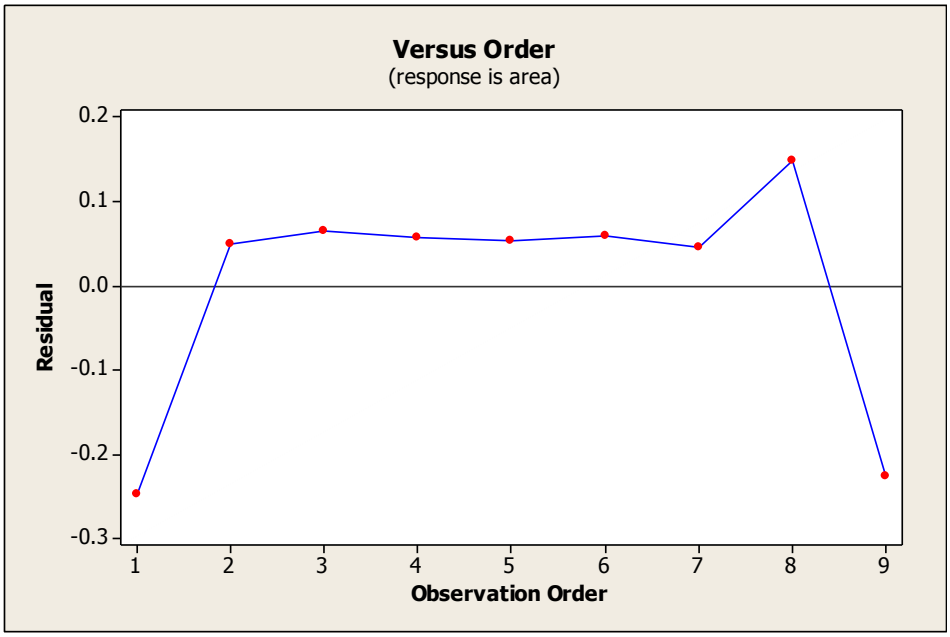

Figure 46. *The values of residual of each point*

From the Figure 44 it can be said that observations 1 and 9, which are the points at times 10 min and 120 min, do not follow the same trend line with the other observations. After the points 1 and 9 have been removed the new graph is plotted with the points from 20 min to 100 min. The new graph is shown in Figure 47.

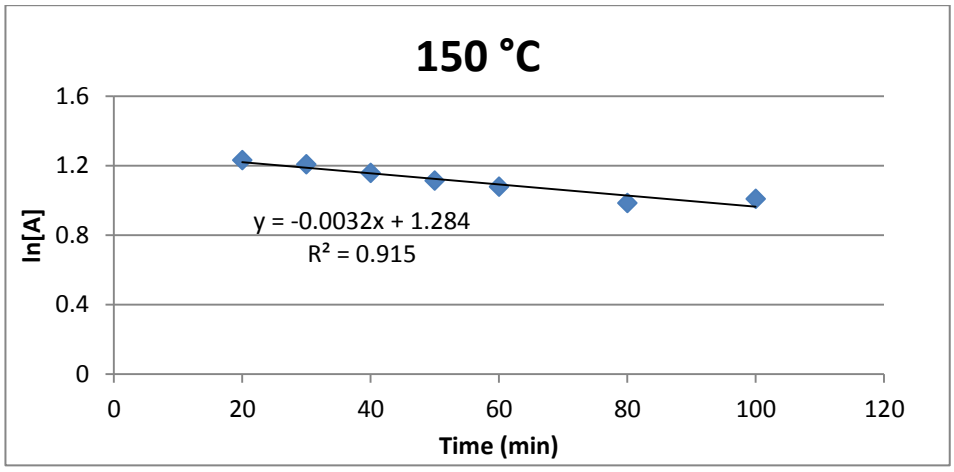

Figure 47. *The new graph of samples measured at 150 °C*

Without the first and last point the correlation coefficient of linear plot increased to 0.915. The peak areas from samples cured at temperatures 160 °C and 170 °C were also plotted in graph. The graphs are shown in Figures 48 and 49.

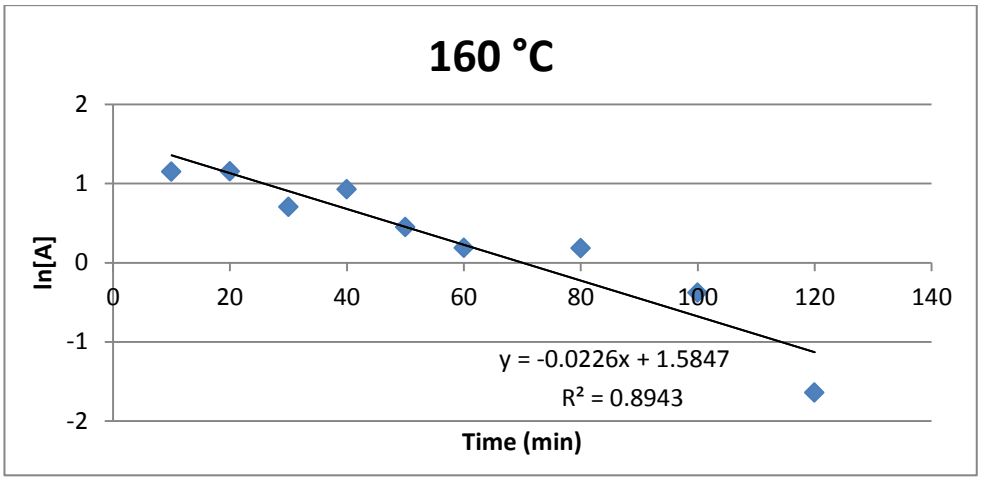

Figure 48. *The graph of samples cured in 160 °C to determine the value for rate constant*

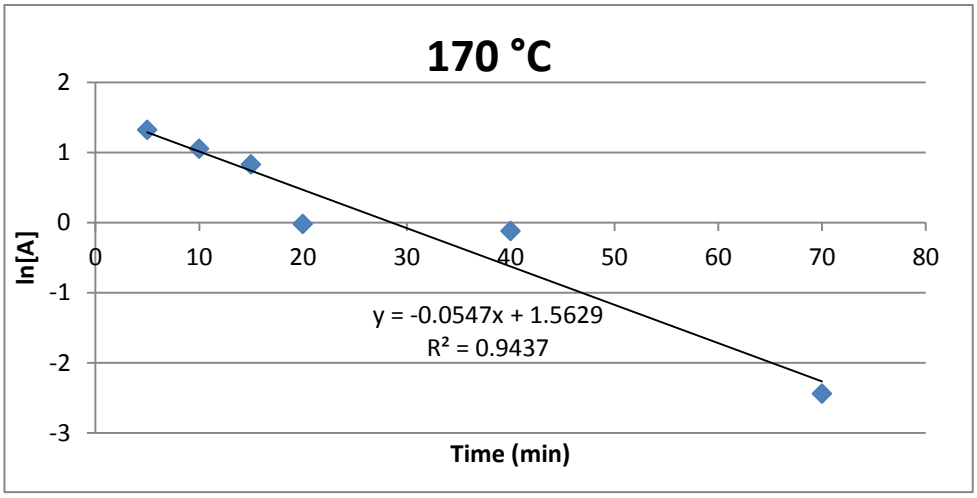

Figure 49. *The graph of samples cured in 170 °C to determine the value for rate constant*

The plots give the rate constant k for each temperature where the peak area was measured. The effect of temperature on the rate constant can be predicted with Arrhenius equation

$$k = Ae^{-\frac{E_A}{RT}} \qquad \text{(eq. 18)}$$

where A is the frequency factor, E_a is the activation energy and R is the universal gas constant. Temperature unit is presented in Kelvins. More convenient way of representing the Arrhenius equation is in logarithmic form

$$lnk = lnA - \frac{E_A}{R}\frac{1}{T} \qquad \text{(eq. 19)}$$

which is the equation of a linear plot whose slope is $-E_A/R$ and the intersection is lnA. This affords a simple way of determining the activation energy from values

of k observed at different temperatures, by plotting lnk as a function of 1/T. [36] (p.15) Values of k from Figures 47, 48 and 49 and temperatures changed to 1/Kelvin units are seen in Table 5.

Table 5. *Values of k from graphs and temperatures changed to 1 per Kelvin units*

Temperature [°C]	1/T (K)	Value of k	ln[k]
150	0.002363228	0.0032	-5.203007187
160	0.002308669	0.0226	-3.789805373
170	0.002256572	0.0547	-2.90589157

Values of k and 1/T from Table 5 are plotted in the graph to calculate the frequency factor A and the activation energy $E_{A.}$ The graph is seen in Figure 50.

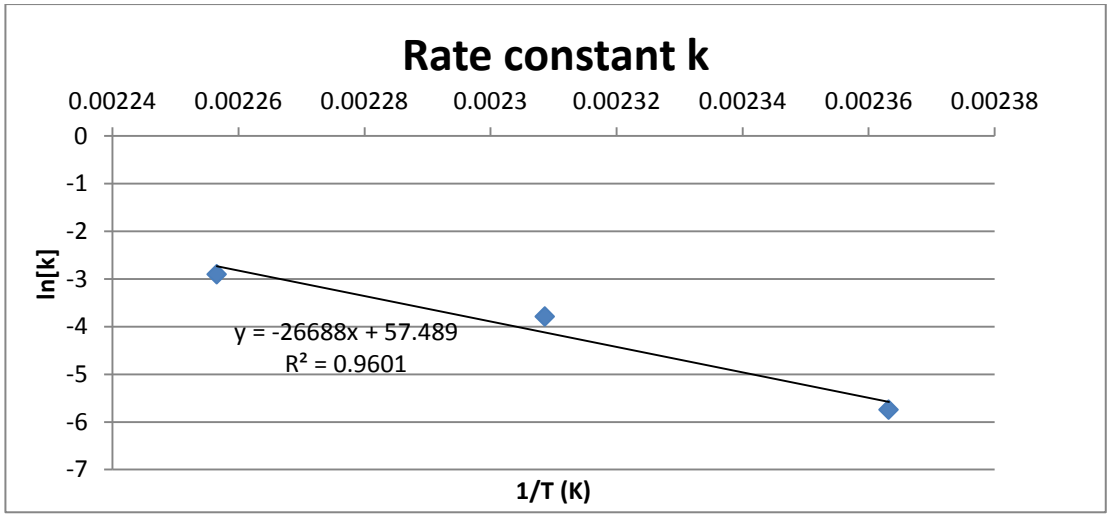

Figure 50. *Rate constant of samples cured at 150 °C, 160 °C and 170 °C*

The slope of the linear plot is the ratio of activation energy E_A and universal gas constant R. The intersection of the slope is the natural logarithm of frequency factor A. The values of these constants are seen in the Table 6.

Table 6. *The values of constants A and E_A/R*

A	**E_A/R**
9.272E+24	26688

The ratio of adhesive after curing A and original adhesive A_0 can be calculated using equation (16). After combining equation (16) and Arrhenius equation (18), the ratio of adhesives is

$$\frac{[A]}{[A_0]} = e^{-Ae^{-\frac{E_A}{RT}}\cdot t} \qquad \text{(eq. 20)}$$

Using the equation (20), the percentage of how much the adhesive changes after curing in different times and temperatures can be calculated as the constants A and E_A/R are known.

6. CONCLUSIONS

The objective of the thesis was to improve knowledge of the properties of a switchable adhesive. The adhesive used in the study was known to switch when heat is applied from PEN film surface to glass. The switching effect is important as the adhesive is used to hold the flexible substrate on the glass carrier as the electronics are fabricated on the flexible substrate and the adhesive should leave no residues to the final product after it has been peeled off from the glass. To study the switching behaviour the adhesive coated on PEN film was laminated on glass slide, cured on different temperatures and peeled.

The surface energy and work of adhesion of the adhesive was studied with using contact angle measurements. The surface energy was found to change when the adhesive laminates were cured above 80 °C. This is the same temperature were the switching from PEN film to glass slide happens. The surface energy of the adhesive changes from ~50 dynes/cm, which is the close to surface energy of PEN film, to ~70 dynes/cm, which is close to the surface energy of glass. The adhesion between two surfaces is stronger when the surface energies are close to each other. The work of adhesion between the adhesive and glass increases when the curing temperature increases above 80 °C. However, when the adhesive was cured in air circulating oven without lamination, the surface energy stayed around 50 dynes/cm. A likely explanation is oxygen inhibition, which causes the decrease in chemical reaction.

The FTIR measurements were made for the same samples used for contact angle measurements. The laminated, cured and peeled adhesive showed a change in spectra in fingerprint region. The peaks at wavenumbers 1060 cm^{-1}, 1150 cm^{-1}, 1175 cm^{-1}, 1243 cm^{-1} and 1269 cm^{-1} were selected for closer study as they were seen to change in the spectra. The peak maximum at 1060 cm^{-1}, which is the C-N stretch, was seen to shift to higher wavenumbers as the curing temperature increased above 160 °C. The double peak area ratio at 1175 cm^{-1} and 1150 cm^{-1}, which both are C-O stretch, was seen to decrease when the curing temperature increased above 160 °C. The same effect was seen with the other double peak at 1243 cm^{-1} and 1269 cm^{-1}, which are also assigned to C-O stretch. The change of peaks after curing temperature increased to 160 °C shows that another change occurs in addition to the switching temperature. The FTIR was also measured of the adhesive samples without lamination. The FTIR spectra did not show a change when the curing temperature increased. These results are consistent with the surface energy results.

The laminates made were peeled and the peel strength measured with 90° peel test after curing the laminates at different temperatures and times. The peel strength was seen to increase when the curing temperature increased to 140 °C. The peel strength increased with higher curing temperatures already after shorter curing times. This indicated that there is a reaction occurring in the adhesive after it is cured above 140 °C. In addition, the peel strength was seen to decrease after laminate was cured at 160 °C for 30 min. With higher curing temperatures the peel strength decreased with a reduction in curing time.

Thermal properties were studied with DSC and TMA. With the DSC the adhesive was heated first to temperatures between 120 °C and 170 °C and the second heating scan was analysed. The adhesive showed an irreversible reaction after 140 °C that was assumed to be due to crosslinking and degradation. The area of reaction peak was calculated with all the samples and the area showed to decrease with increased heating temperature and time. This reaction is most likely the same as the reaction detected with FTIR and peel tests. Also a melt peak was observed at temperature around 125 °C. The area of melt peak was seen to decrease when the first heat increased to 150 °C and it was kept there for longer times. In addition, the glass transition temperature of the adhesive was analysed with DSC. The T_g was seen with first heating at temperature between -50 °C and -40 °C. With the second heating the T_g could not be seen. The TMA showed softening of the adhesive after -20 °C and therefore the T_g is at lower temperatures which is consistent with the findings from DSC analysis. In addition, with TMA the adhesive was found to soften at higher temperatures after the first heating so it was assumed that the glass transition temperature also shifts to a higher temperature in the second heating run.

Two changes were detected to occur in the adhesive after curing. The first change occurs around 80 °C where the adhesive is seen to switch from the PEN film to glass after peeling. The change can be also seen with surface energy measurements where the surface energy of the adhesive changes from 50 dynes/cm to 70 dynes/cm after curing it around 80 °C. However, the change not occur when the adhesive is cured in air, because the oxygen inhibition.

Another change takes place around 140 °C depending on the curing time and measuring technique. This change is detected with FTIR, peel tests and DSC. The change is most likely due with the crosslinking and degradation and it is an irreversible reaction. The kinetics of this reaction was calculated using peak areas measured with FTIR. With the kinetics calculation the percentage change in the adhesive with any curing time and temperature can be calculated. In further work, the kinetics of the adhesive could also be calculated using the DSC data. A detailed analysis of the chemical composition of the adhesive and the mechanisms of the chemical change which occur during curing is largely beyond the scope of this thesis. Some insight has been provided using FTIR,

surface energy and thermal measurements. However more understanding and research in this area would be very valuable.

REFERENCES

[1] Brydson, J.A. Polyesters. In: Anonymous (ed.). Plastics Materials. 7th ed. 1999, Butterworth Heinemann. pp. 694-743.

[2] Brooks, D. & Giles, G. PET packaging technology. Sheffield 2002, Sheffield Academic Press Ltd. 375 p.

[3] Fakirov, S. (ed.). 2002. Handbook of Thermoplastic Polyesters, Volume 1. Weinheim, Wiley-VCH. 753 p.

[4] MacDonald, W.A. Polyester Films. In: Anonymous (ed.). Encyclopedia of Polymer Science and Technology. 3rd ed. 2002, John Wiley & Sons. pp. 30-41.

[5] Process flow. Ampef. 2002, [accessed on 2/2015]. Available: http://www.ampef.com/technology2.html.

[6] Choi, M.-., Kim, Y. & Ha, C.-. Polymers for flexible displays: From materials selection to device applications. 33(2008) pp. 581-630.

[7] Flexible OLEDs: introduction, applications and market status. OLED info. [accessed on 2/2015]. Available: http://www.oled-info.com/flexible-oled.

[8] DuPont Teijin Films Teonex® PEN Film for Flexible Displays and Electronics. DuPont. 2014, [accessed on 2/2015]. Available: http://corian.hu/Displays/en_US/products_services/films/PEN_film.html.

[9] A.J. Kinloch Adhesion and adhesives: Science and Technology. London 1987, Chapman and Hall. 441 p.

[10] Benedek, I. & Heymans, L.J. Pressure-sensitive Adhesives Technology. New York 1997, Marcel Dekker Inc. 600 p.

[11] de Crevoisier, G., Fabre, P., Corpart, J.-. & Leibler, L. Switchable Tackiness and Wettability of a Liquid Crystalline Polymer. Science 20 285(1999) pp. 1246-1249.

[12] Gurney, R.S., Dupin, D., Nunes, J.S., Ouzineb, K., Siband, E., Asua, J.M., Armes, S.P. & Keddie, J.L. Switching Off the Tackiness of a Nanocomposite Adhesive in 30 s via Infrared Sintering. Applied Materials and Interfaces (2012) pp. 1-36.

[13] Miller, M., MacDonald, W. & Adam, R. Adhesion of UV-Cured Laminates of Poly(ethylene-2,6-naphthalene) (PEN) and Poly(ethylene terepthalate) (PET) films. 26(2012)1-3, pp. 55-78.

[14] Cho, A., Kim, E., Park, S. & Park, L. Flexible OLED encapsulated with gas barrier film and adhesive gasket. 193(2014) pp. 77-80.

[15] MacDonald, W.A. Engineering films for display technologies. Journal of Material Chemistry 14(2004) pp. 4-10.

[16] Haq, J., Vogt, B., Raupp, G. & Loy, D. Impact of adhesive rheology on stress-distortion of bonded plastic substartes for flexible electronics applications. Microelectronic Engineering 88(2011) pp. 2852-2856.

[17] Future of OLEDs. Novaled. 2015, [accessed on 2/2015]. Available: http://www.novaled.com/oleds/future_of_oleds/.

[18] Krol, P. & Krol, B. Determination of free surface energy values for ceramic materials and polyurethane surface-modifying aqueous emulsions. Journal of the European Ceramic Society 26(2006) pp. 2241-2248.

[19] Carre, A. Polar interactions at liquid/polymer interfaces. Journal of Adhesion Science Tehnology 21(2007)10, pp. 961-981.

[20] Shimizu, R.N. & Demarquette, N.R. Evaluation of surface energy of solid polymers using different models. Journal of Applied Polymer Science 76(2000) pp. 1831-1845.

[21] Wu, S. Calculation of interfacial tension in polymer systems. Journal of Polymer Science, Part C 34(1971) pp. 19-30.

[22] Schrader, M.E. Young- Dupre Revisited. Langmuir 11(1995)9, pp. 3585-3589.

[23] Zenkiewicz, M. Methods for the calculation of surface free energy of solids. Journal of Achievements in Materials and Manufacturing Engineering 24(2007)1, pp. 137-145.

[24] Alvarez-Ordonez, A. & Prieto, M. Fourier transform Infrared Spectroscopy in Food Microbiology. New York 2012, Springer US. 54 p.

[25] Glassford, S.E., Byrne, B. & Kazarian, S.G. Recent applications of ATR FTIR spectroscopy and imaging to proteins. Biochimica et Biophysica Acta 1834(2013) pp. 2849-2858.

[26] Alvarez-Ordóñez, A., Mouwen, D.J.M., López, M. & Prieto, M. Fourier transform infrared spectroscopy as a tool to characterize molecular composition and stress response in foodborne pathogenic bacteria. Journal of Microbiological Methods 84(2011) pp. 369-378.

[27] Gardon, J.L. Peel Adhesion. I. Some Phenomenological Aspects of the Test. Journal of Applied Polymer Science 7(1963) pp. 625-641.

[28] Ehrenstein, G.W., Riedel, G. & Trawiel, P. Thermal Analysis of Plastics: Theory and Practice. Munchen 2004, Carl Hanser Verlag. 368 p.

[29] Menard, K.P. Thermomechanical and Dynamic Machanical Analysis. In: Lobo, H. & Bonilla, J.V. (ed.). Handbook of Plastics Analysis. New York 2003, Marcel Dekker Inc. pp. 155-200.

[30] Corcione, C.E. & Frigione, M. Factors influencing photo curing kinetics of novel UV-cured siloxane-modified acrylic coatings: oxygen inhibition and composition. Thermochimica Acta 534(2012) pp. 21-27.

[31] Husar, B., Ligon, S.L., Wutzel, H., Hoffmann, H. & Liska, R. The formulator's guide to anti-oxygen inhibition additives. Progress in Organic Coatings 77(2014) pp. 1789-1798.

[32] Coates, J. Interpretation of Infrared Spectra. In: Meyers, R.A. (ed.). Encyclopedia of Analytical Chemistry. 2000, John Wiley & Sons Ltd. pp. 10815-10837.

[33] Williams, J.A. & Kauzlarichb, J.J. The influence of peel angle on the mechanics of peeling flexible adherends with arbitrary load–extension characteristics. Tribology International 38(2005-2006)11-12, pp. 951-958.

[34] Earnest, C.M. Assignment of the Glass Transition Temperatures Using Thermomechanical Analysis. In: Seyler, R.J. (ed.). Assignment of the Glass Transition. Philadelphia 1994, American Society for Testing and Materials. pp. 75-87.

[35] Mijovic, J. & Andjeli, S. A Study of Reaction Kinetics by Near-Infrared Spectroscopy. 1. Comprehensive Analysis of a Model Epoxy/Amine System. Macromolecules 28(1995) pp. 2787-2796.

[36] Perry, R.H. & Chilton, C.H. Reaction Kinetics, Reactor Design and Thermodynamics. In: Anonymous (ed.). Chemical Engineers' Handbook. 5th ed. 1973, Mcgraw-Hill Kogakusha Ltd. pp. 1-75.

[37] Gobrecht, A., Bendoula, R., Roger, J.-. & Bellon-Maurel, V. Combining linear polarization spectroscopy and the Representative Layer Theory to measure the Beer-Lambert law absorbance of highly scattering materials. Analytica Chimica Acta 853(2015) pp. 486-494.